Quaternary Science Reviews 28 (2009) 1434–1448

Contents lists available at ScienceDirect

Quaternary Science Reviews

journal homepage: www.elsevier.com/locate/quascirev

Vegetation change, goats, and religion: a 2000-year history of land use in southern Morocco

Helen V. McGregor[a,b,*], Lydie Dupont[a], Jan-Berend W. Stuut[a], Holger Kuhlmann[a]

[a] MARUM—Center for Marine Environmental Sciences, University of Bremen, Leobener Strasse, D-28359 Bremen, Germany
[b] School of Earth and Environmental Sciences, Northfields Avenue, University of Wollongong, Wollongong, NSW 2522, Australia

ARTICLE INFO

Article history:
Received 26 September 2008
Received in revised form
12 February 2009
Accepted 18 February 2009

ABSTRACT

Understanding past human–climate–environment interactions is essential for assessing the vulnerability of landscapes and ecosystems to future climate change. This is particularly important in southern Morocco where the current vegetation is impacted by pastoralism, and the region is highly sensitive to climate variability. Here, we present a 2000-year record of vegetation, sedimentation rate, XRF chemical element intensities, and particle size from two decadal-resolved, marine sediment cores, raised from offshore Cape Ghir, southern Morocco. The results show that between 650 and 850 AD the sedimentation rate increased dramatically from 100 cm/1000 years to 300 cm/1000 years, and the Fe/Ca and pollen flux doubled, together indicating higher inputs of terrestrial sediment. Particle size measurements and end-member modelling suggest increased fluvial transport of the sediment. Beginning at 650 AD pollen levels from Cichorioideae species show a sharp rise from 10% to 20%. Pollen from *Atemisia* and *Plantago*, also increase from this time. Deciduous oak pollen percentages show a decline, whereas those of evergreen oak barely change. The abrupt increase in terrestrial/fluvial input from 650 to 850 AD occurs, within the age uncertainty, of the arrival of Islam (Islamisation) in Morocco at around 700 AD. Historical evidence suggests Islamisation led to population increase and development of southern Morocco, including expanded pastoralism, deforestation and agriculture. Livestock pressure may have changed the vegetation structure, accounting for the increase in pollen from *Cichorioideae*, *Plantago*, and *Artemisia*, which include many weedy species. Goats in particular may have played a dominant role as agents of erosion, and intense browsing may have led to the decline in deciduous oak; evergreen oak is more likely to survive as it re-sprouts more vigorously after browsing. From 850 AD to present sedimentation rates, Fe/Ca ratios and fluvial discharge remain stable, whereas pollen results suggest continued degradation. Pollen results from the past 150 years suggest expanded cultivation of olives and the native argan tree, and the introduction of Australian eucalyptus trees. The rapidly increasing population in southern Morocco is causing continued pressure to expand pastoralism and agriculture. The history of land degradation presented here suggests that the vegetation in southern Morocco may have been degraded for a longer period than previously thought and may be particularly sensitive to further land use changes. These results should be included in land management strategies for southern Morocco.

1. Introduction

Late Quaternary records of climate change, human activity, and vegetation response are recognised as essential to understanding present and future interactions of these systems (Dearing et al., 2006). Records of past climate–human–environment interactions not only provide a 'baseline' for comparison with the present, but can be used to understand landscape/ecosystem thresholds, the complex, non-linear behaviour of these systems, and can be utilised to develop more appropriate conservation and land management strategies (Dearing, 2006; Froyd and Willis, 2008). A key concept in climate–human–environment interactions is to use knowledge of the past to assess the resilience of natural systems to future change (Dearing, 2008).

Assessing resilience is of particular importance to countries such as Morocco, a country presently subject to desertification and land degradation (Mikesell, 1960; Puigdefábregas and Mendizabal, 1998), and likely to face increased climate variability, socio-economic stressors, and population pressure in the future (Agoumi, 2003; Giorgi, 2006; Christensen et al., 2007). Studies of Moroccan climate, vegetation and landscape changes for the Late Quaternary

* Corresponding author. School of Earth and Environmental Sciences, Northfields Avenue, University of Wollongong, Wollongong, NSW 2522, Australia. Tel.: +61 2 4221 4265; fax: +61 2 4221 4250.
E-mail address: mcgregor@uni-bremen.de (H.V. McGregor).

0277-3791/$ – see front matter Crown Copyright © 2009 Published by Elsevier Ltd. All rights reserved.
doi:10.1016/j.quascirev.2009.02.012

have focused on the northern regions of the country. Lake records from the Middle Atlas, northern Morocco, suggest predominantly climatic influences on vegetation and lake levels through the Holocene until 3.0–2.0 thousand years before present (ka BP) (Lamb et al., 1995; Cheddadi et al., 1998). From this period however, signs of deforestation are inferred from pollen and sedimentation rates (Lamb et al., 1991, 1999). From 1.8 to 1.0 ka BP (150–950 AD), sedimentation rates increase further and weedy species appear, suggesting more intensive cultivation and modification of the landscape (Lamb et al., 1991). In contrast, the vegetation history of the southern Moroccan is largely unknown. This is despite studies of the present-day vegetation in this region suggesting the landscape is strongly degraded by deforestation and the browsing of goats (Barbero et al., 1990; Culmsee, 2004).

In this study, we present a 2000-year history of vegetation and terrestrial change for southern Morocco, using pollen, particle size, and element intensity records from two marine sediment cores raised from the southern Moroccan continental margin (Fig. 1). We investigate human–environment interactions in this sensitive region, and build on previous research into the paleoclimate signal recorded in the cores (McGregor et al., 2007). The primary sediment core used in this study, GeoB 6008-1, is unusual in that it has near-decadal resolution, excellent age control, and extending well into the late 20th Century. The results from the GeoB 6008-1 show that from ~650 to 850 AD there is an abrupt change to increased sedimentation rates, most likely due to increased fluvial input, and concurrent changes in the pollen record. By comparing these results to other pollen and paleoclimate records from Morocco, and to documented Moroccan historical events, we explore the possible climate and/or human-induced origin of this abrupt shift and discuss the implications for current land use trends in Morocco.

2. Regional setting

2.1. The climate of Morocco

Much of southern Morocco is classed as arid to semi-arid. Rainfall in low-lying regions is 200–300 millimetres per annum (mm/a; arid), and mountainous regions receive 400–600 mm/a (semi-arid; Till and Guiot, 1990; Knippertz et al., 2003; Weisrock et al., 2006). There is also a north–south precipitation gradient, with regions north of 32°N receiving 400–800 mm/a (semi-arid to sub-humid) and regions south receiving 200–600 mm/a (arid to semi-arid; Till and Guiot, 1990). Precipitation falls almost entirely in the boreal winter, and in the High Atlas it falls as snow (Knippertz et al., 2003; Weisrock et al., 2006). Precipitation in the northern and western parts of Morocco, including the High Atlas, is controlled by variations in the North Atlantic Oscillation (NAO); when NAO is in a negative mode winter rainfall increases (Knippertz et al., 2003). The NAO has been recognised as a major atmospheric circulation

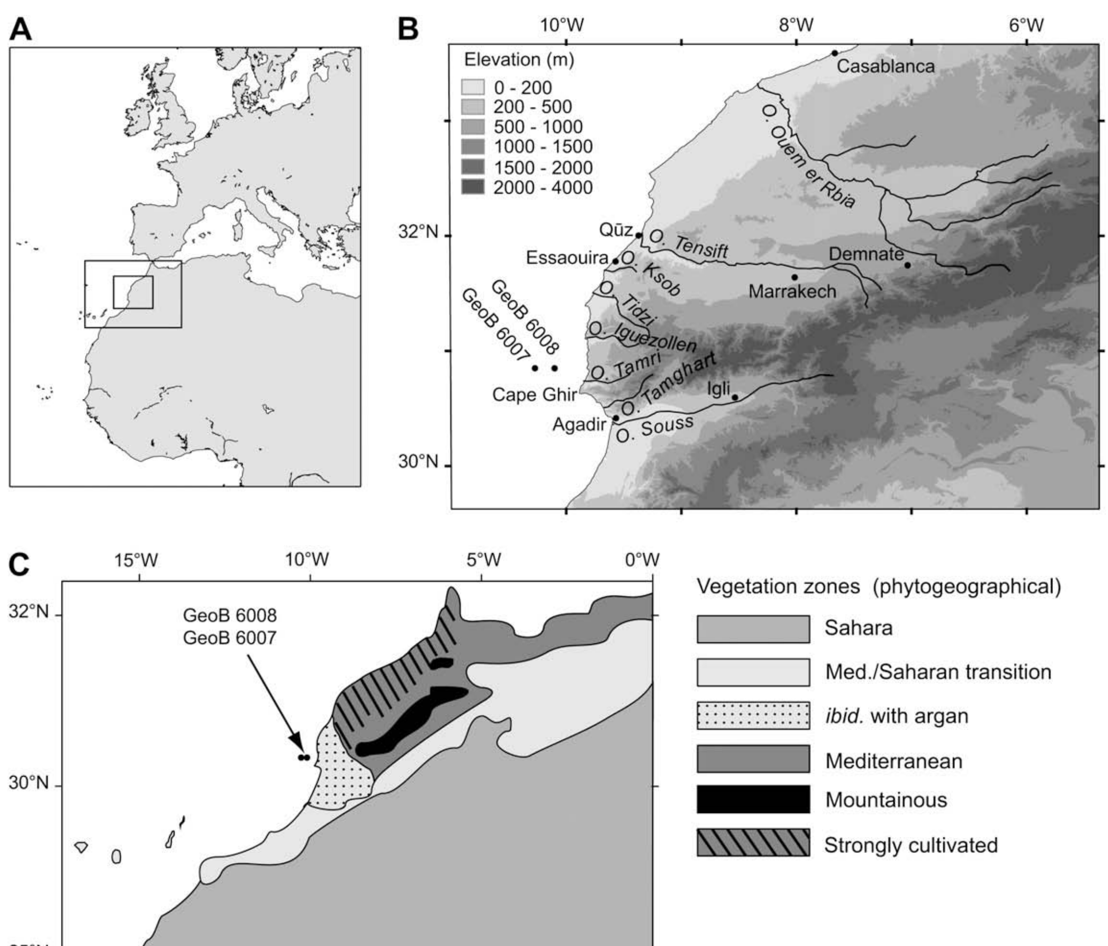

Fig. 1. Topographic map of the southern Morocco region, and major vegetation zones for NW Africa. (A) Overview of the European-West African region. Small box indicates the region represented in (B), and the large box shows the area covered in (C). (B) Southern Morocco topographical map. The location of sediment core Sites GeoB 6008 and GeoB 6007 are indicated, as are the major rivers draining the High Atlas and Anti Atlas Mountains. (C) Major vegetation zones for NW Africa, modified after White (1983). Pollen types associated with the vegetation zones are given in Table 1.

pattern influencing Moroccan winter precipitation over at least the past 500 years (Pauling et al., 2006). Tree ring width data used to reconstruct the Palmer Drought Severity Index for Morocco for the past ~1000 years further suggests a strong relationship between Moroccan drought conditions and large-scale atmospheric circulation patterns (Esper et al., 2007). On millennial time scales, NAO mechanisms are thought to influence Moroccan precipitation and fluvial runoff (Kuhlmann et al., 2004b).

2.2. Modern vegetation zonation

The vegetation of Morocco belongs to the (1) Mediterranean, (2) Mediterranean–Saharan transition, and (3) Saharan phytogeographical zones (Table 1, Fig. 1C; Quézel, 1978; White, 1983; Benabid, 1985). The Mediterranean vegetation zone consists of forests, bushland and thickets, shrublands, and mattoral; the humid forests include firs (*Abies maroccana*), cedars (*Cedrus atlantica*), and deciduous oaks (*Quercus faginea*, *Q. pyrenaica*); drier forests include evergreen oaks (*Q. rotundifolia*, *Q. ilex*, *Q. suber*, *Q coccifera*), olives (*Olea europaea*), gharghar tree (*Tetraclinis articulata*), junipers (*Juniper phoenicea*), and pines (*Pinus halepensis*, *P. pinaster*) (English names according to The Plant Press, 1997–2006). *Pistacia atlantica*, *Juniperus phoenicea*, *J. thurifera*, *Fraxinus dimorpha*, *Argania spinosa* (argan tree), and acacia trees (*Acacia gummifera*, *A. raddiana*, *A. ehrenbergiana*) are constituents of bushland and shrubland. Mattoral or maquis is a community of drought tolerant plants dominated by shrubs that grow in arid regions that are hot and dry in summer and cool and moist in winter.

The Mediterranean–Saharan transition zone includes the argan scrub forest and *Stipa* (esparto) steppes. The argan tree (*Argania spinosa*) is endemic to southwest Morocco and produces an edible, valuable oil.

The Saharan zone consists of sparse desert vegetation with Chenopodiaceae, grasses, acacia trees (*A. raddiana*, *A. ehrenbergiana*), *Balanites aegytiaca* (desert date), *Capparis decidua*, *Maerua crassifolia*, *Tamarix articulata*, and *Rhus tripartita* growing localized on salty soils, on dunes, and in wadis.

Degradation characterises much of the present day vegetation in Morocco and proceeds through a number of stages (Barbero et al., 1990). In the first stage sclerophyllous species invade the more humid forest. Next scrubs and small trees are replaced by shrubs, which may be followed by a process known as steppisation (invasion of steppe-like vegetation elements). During steppisation the wooded vegetation is replaced by either Scrophulariaceae and Lamiaceae (thyme species), by the woody Asteraceae, *Artemisia* and *Launaea*, or by grasses like *Stipa* (esparto). The final step in the degradation of the vegetation includes further invasion of grasses and Asteraceae species with short generation periods, which only grow during advantageous seasons or periods. Any trees in this type of degraded vegetation are leftovers that cannot renew themselves, eventually dying out. The argan scrub forest in the Souss River region (south of our study area) are currently in this state (Barbero et al., 1990).

Immediately landward of our core location vegetation is dominated by the argan scrub forest sub-zone and further inland the mountain steppe sub-zone of the western High Atlas (Benabid, 1985), which together represent important source of pollen grains to Site GeoB 6008. Culmsee (2004) studied specifically the modern vegetation of the western High Atlas directly onshore from Site GeoB 6008: at low altitudes near the coast, *Argania spinosa* (argan) scrubs, and shrubs such as *Euphorbia beaumeriana* and *Periploca laevigata* (wolfbane), are found. Further inland *Argania spinosa* (argan tree) is accompanied by the bushes *Epherda fragilis* (joint pine), *Launaea arborescens*, *Olea europaea* ssp. *maroccana* (wild olive tree), *Tetraclinis articulata* (gharghar tree), and *Pistacia lentiscus* (mastic tree). The understorey consists of *Phillyrea angustifolia* bushes (jasmine box) growing with *Stipa tenacissima* (esparto grass), or with *Chamaerops humilis* (European fan palm) and *Brachypodium retusum* (Mediterranean false brome). At altitudes of 1400–1800 m *Juniperus oxycedrus* (sharp cedar) and *Quercus rotundifolia* (holm oak or evergreen oak) are found in some cases together with *Pistacia lentiscus* trees, *Phillyrea angustifolia* shrubs, and *Bupleurum atlanticum* herbs.

Table 1
Selected vegetation zones shown in Fig. 1C and pollen taxa associated with each zone (after Hoogheimstra et al. (1992), with additions after Benabid (1985)).

Vegetation zones	Pollen taxa
Mediterranean	
Conifer forest	*Abies*, *Cedrus*, *Juniperus*, *Pinus*, *Tetraclinis*
Deciduous oak forest	*Q. robur/pubescens*-type
Evergreen oak forest	*Q. cerris/ilex*-type
Bushland and thicket	*Ceratonia*, *Jasminum*, *Juniperus*, *Tetraclinis* *Olea*, *Phillyrea*, *Pistacia*, *Q. cerris/ilex*-type, *Rhamnus*, *Rhus*, *Ephedra*
Mattoral (anthropogenic)	*Arbutus*, *Cistus*, *Erica*, *Juniperus*, *Olea*, *Phillyrea*, *Pistacia*, *Q. cerris/ilex*-type
Mountainous shrubland	*Artemisia*, *Juniperus*, *Ephedra*
Coastal dunes	*Euphorbia*
Salt marshes	Chenopodiaceae, Plumbaginaceae, Asteroideae, *Artemisia*
Mediterranean–Saharan transition	
Argan scrub forest	*Argania spinosa*, *Euphorbia*, *Tetraclinis*, *Juniperus*, *Ziziphus*, *Pistacia*, Cichorioideae (*Launaea*)
Steppes	*Stipa* (grass pollen), *Artemisia*, *Ephedra*, *Plantago*
On salt soils	Chenopodiaceae
Saharan	
Wadis	*Acacia*, *Panicum* (grass pollen), *Tamarix*
Dunes	*Aristida* (grass pollen), *Calligonum*, *Ephedra*, *Plantago*
Desert	Chenopodiaceae

Pollen types may originate from more than one vegetation zone.

3. Methods

3.1. Core location and age model

The 5.3 m-long gravity core GeoB 6008-1, and 0.33 m-long multi-core (MUC) GeoB 6008-2 were retrieved during METEOR cruise M 45/5, from the continental slope off Cape Ghir, Morocco (30°50.7′ N, 10°05.9′ W) in 355 m water depth (Fig. 1; Neuer and cruise participants, 2000). The age model for gravity core GeoB 6008-1 is based on 17 ^{210}Pb and 8 AMS ^{14}C age determinations, and bomb fallout ^{137}Cs was used to cross-check the ^{210}Pb age model (McGregor et al., 2007). Radiocarbon dates are based on measurement of 1000–1500 *Globigerina bulloides* (>150 μm fraction) per sample. The core extends from 520 BC to 1977 AD and the age model suggests an extremely high average sedimentation rate of ~210 cm/1000 years, with a sedimentation rate change to increased sedimentation, defined by three of AMS ^{14}C dates, calibrated to 551(670)789, 700(835)986 and 797(980)1084 AD (2σ age ranges). The visual core description and colour measurements of GeoB 6008-1 show no obvious lithological disturbances or diagenetic overprint in the cores. The sedimentation rate change however, occurs at the same time as a colour shift from olive brown to dark yellowish brown sediments (Neuer and cruise participants, 2000). The age model for MUC GeoB 6008-2 is based on 32 ^{210}Pb dates and extends from 1912 to 1998 AD (McGregor et al., 2007).

Core GeoB 6008-1 was scanned by XRF for element intensities, and samples were taken for pollen and particle size analysis. Samples from GeoB 6008-2 were analysed for particle size.

3.2. X-ray fluorescence (XRF) methods

Down-core element intensities for Ca, Fe, K, Ti and Al were obtained from gravity core GeoB 6008-1 using the non-destructive XRF Core Scanner II housed at the University of Bremen. The Core Scanner was run with an excitation potential of 10 kV, 30 s count time and, an X-ray current of 350 μA. The step interval was 1 cm. The resulting data are element intensities. Data were normalised by dividing the total counts for each element by the summed total counts of all measured elements. In general, Ca is considered a proxy for marine productivity, whereas Fe, K, Ti and Al are proxies for the terrestrial environment (see Sections 4 and 5 for details).

3.3. Particle size analysis and end-member modelling

The down-core sampling interval of GeoB 6008-1 was between 2 cm and 10 cm, which took into account the change in sedimentation rate between 650 and 850 AD, and gave a sample resolution of 40 years per sample before 400 AD and 30 years per sample after 400 AD. GeoB 6008-2 was sampled at 5 cm intervals, which gave an average resolution of 14 years per sample.

Biogenic constituents were removed from GeoB 6008-1 and GeoB 6008-2 sediment core samples to isolate the terrigenous fraction prior to particle size analysis. First, to remove organic carbon (C_{org}), 10 ml H_2O_2 (35%) was added to approximately 750 mg of bulk sediment and the mixture was boiled until the reaction ceased and excess H_2O_2 disintegrated into H_2O and O_2. Next, to remove calcium carbonate 10 ml HCl (10%) in 100 ml demineralised water was added to the sediment and boiled for one minute to speed up the reaction. Visual checks were made to ensure the removal of all $CaCO_3$. The sediment was then diluted with demineralised water until approximately neutral pH was achieved. As a last pre-treatment step biogenic silica was removed; 6 g of NaOH pellets dissolved in 100 ml demineralised water was added to the sediment and the mixture was boiled for 10 min. Visual checks were made periodically to ensure the removal of all diatoms and radiolarians. The solution was diluted with demineralised water to a neutral pH. Immediately prior to particle size analysis, the now C_{org}-, $CaCO_3$-, and biogenic opal-free sediment (i.e. terrigenous fraction) was boiled with 300 mg of the soluble salt sodium pyrophosphate ($Na_4P_2O_7 \cdot 10H_2O$) to ensure disaggregation of all particles.

Particle size distributions of the terrigenous fraction were measured with a Coulter laser particle sizer LS200, which resulted in 92 size classes from 0.4 to 1908 μm. Approximately 10 ml of sediment was collected from cores GeoB 6008-1 and GeoB 6008-2.

The end-member modelling technique was then applied to the measured particle size distributions, to determine the proportions of distinct sediment components contributing to the overall, measured particle size signal (Weltje, 1997). In general, the terrigenous fraction of deep-sea sediments in the (sub)tropical ocean that are not disturbed by post-depositional processes can be considered a mixture of aeolian and fluvial sediments. Using the end-member algorithm, particle size distributions of deep-sea sediments can successfully be 'unmixed' into subpopulations, or end-members, (Weltje, 1997). These end-members can then be related to sediment transport mechanisms, for example, increases in aeolian end-members could be related to changes in wind conditions (Prins and Weltje, 1999; Stuut et al., 2002; Arz et al., 2003; Frenz et al., 2003; Weltje and Prins, 2003; Holz et al., 2004).

The end-member modelling technique uses an algorithm that describes the variance in any given dataset. The only prescription of the technique is that end-members may not have negative particle sizes. No predefinitions are made regarding shape, sorting or modal sizes of the end-members (for more details of the application of the model to particle-size distributions see Weltje and Prins, 2003). The algorithm output is a series of models, with each containing a different number of 'end-members', and each model explaining a different amount of variance; the higher the number of end-members the more variance explained. Two key parameters, calculated from the end-member algorithm goodness-of-fit statistics, are used to determine the minimum number of end-members required for a satisfactory approximation of the measured data (Weltje, 1997; Prins and Weltje, 1999). First, the coefficient of determination per size class (r^2) is used to assess how well the model reproduces the data in each size class. Second, the mean coefficient of determination averaged for all size classes (r^2_{mean}) is used to test overall how well each model reproduce the average of all measured size classes. The r^2_{mean} increases when the number of end-members per model increases. However r^2_{mean} may average out instances where an individual size class has a low r^2 (hence taking into account r^2 is also important). The final end-member model used to explain the data and determine transport mechanisms represents the best compromise between the number of end-members in the model (i.e. highest possible r^2_{mean}) and highest r^2 for each size class, that is, the optimal balance between statistical description of the variance in the data set and complexity of mixture compositions. The eventual outcome of the algorithm is a statistically unique solution (model) with end-members (subpopulations) that represent real particle-size distributions.

3.4. Pollen preparation and analysis

Samples of 3–10 ml were taken from core GeoB 6008-1. The sampling interval was 5–10 cm from 50 AD to 1100 AD, then every 40 cm to the core top. This sampling interval takes into account the change in sedimentation rate between 650 and 850 AD. The sampling interval is equivalent to 30–60 years/sample between 500–1200 AD, and up to 120 years/sample before and after this period. Sample preparation follows standard procedures (Faedri and Iversen, 1989; Moore et al., 1991) with some deviations as noted. The actual volume of each sample was measured by water displacement. Samples were decalcified in diluted HCl (droplets of ca. 12% HCl were added to the sample) and *Lycopodium* tablets containing a known number of marker spores were added. After washing and centrifuging, 48% HF was added up to a doubling of the volume. Samples were kept in the HF solution for at least two days. After neutralising with 40% KOH, and subsequent washing with water, the >10 μm clay and organic debris fraction, was removed by ultrasonic sieving using a mesh of 8 μm. The final residue was stored in water. Microscope slides were made of the residue and were mounted in glycerol.

Slides were then examined with a light microscope using a magnification of 400× or 1000×. Three to four hundred pollen grains were counted for each sample. Two to three hundred dinoflagellate cysts per sample were also counted. The pollen percentages are based on the total counts of pollen.

Pollen was identified using the pollen identification key of the African Pollen Database reference collection http://medias.obs-mip.fr/pollen/, and after Beug (2004). With a few exceptions determination of pollen is to genus or family level. Fenestrate pollen were counted as Cichorioideae pollen. Two types of *Quercus* pollen grains were determined, *Quercus cerris/ilex*-type and *Quercus robur/pubescens*-type. The *Q. cerris/ilex*-type contains pollen from evergreen oaks (*Q. rotundifolia*, *Q. ilex*, *Q. coccifera*, *Q. suber*);

Q. robur/pubescens-type pollen from deciduous oaks. Two types of *Ephedra* pollen grains were determined, *E. fragilis*-type and *E. distachya*-type. The *Ephedra fragilis*-type is more common in marine surface sediments off NW Africa between 35° and 23° N reaching 2–5%, whereas *E. distachya*-type pollen grains are rare in marine surface sediments, not exceeding 1% (Hooghiemstra et al., 1986). The distribution patterns of both *Ephedra* pollen types in marine surface sediments closely matches the average wind flow pattern of the NE trade winds, and the representation maximum correlates with the latitude of main distribution of *Ephedra* species on land (Hooghiemstra et al., 1986). Thus percentages of *E. distachya*-type and *E. fragilis*-type are summed, and in terms of spatial distribution in marine sediments these pollen types are considered together.

4. Results

4.1. XRF results

Ca intensity shows highest values (mean 0.54) compared to all elements measured (Fig. 2A). The second highest mean intensity was for Fe, with 0.28, and the third was K with 0.09 (Fig. 2A). All other elements have mean intensities of less than 0.04.

Ca intensity, while clearly the most intense of the core, show a ~25% reduction between 650 and 850 AD and this reduction is sustained to the present. At the same time Fe and K show a rapid increase to a consistently higher level. This abrupt shift is highlighted by Fe/Ca and K/Ca ratios (Fig. 2B) and is a robust feature of the XRF results from this core; log ratio plots of the XRF data (not shown) also show an abrupt shift in Ca and Fe between 650 and 850 AD. The variability in the most recent 1000 years for all elements and ratios appears to increase, however this is most likely an artefact of the increased resolution (higher sedimentation rate) of the sediment core after 650 AD.

Ca intensities are interpreted as representing the carbonate component deposited at the site, and given that the core is located in the heart of the highly productive Cape Ghir upwelling centre (McGregor et al., 2007), most likely represents marine productivity (Kuhlmann et al., 2004a). K in marine sediment cores is generally associated with terrestrial siliciclastics (e.g. illite clays and potassium feldspar; Martinez et al., 1999; Yarincik et al., 2000). Fe intensities also represent terrestrial input, in this case possibly as iron oxyhydroxides. The Ti record (not shown) mirrors the Fe pattern. Ti is much less susceptible to diagenesis than Fe, so the similarity between the Fe and Ti records suggests that the Fe record is unlikely to be the result of a diagenetic overprint. Overall, the changes in Ca, Fe and K at 650–850 AD most likely represent a relative decrease in marine productivity and/or a relative increase in terrestrial material reaching the site.

Previous studies have linked Al in sediment cores to intense chemical weathering on land producing kaolinite and smectite clays (Yarincik et al., 2000; Zabel et al., 2001) and the K/Al ratio reflects the intensity of the weathering process (higher Al equates to more intense weathering). Increases in the Ti/Al ratio are thought to reflect aeolian input (Yarincik et al., 2000). The K/Al and Ti/Al ratios show little change in mean values down core (Fig. 2B).

4.2. Particle size and end-member modelling results

The median particle size distribution of the silt fraction in cores GeoB 6008-1 and GeoB 6008-2 ($N = 83$) has a modal particle size near 10 μm (Fig. 3A). The median particle size shows a dramatic decrease between 650 and 850 AD (Fig. 3B), and this shift occurs at the same time as the changes seen in Ca, Fe and K intensities (Fig. 2).

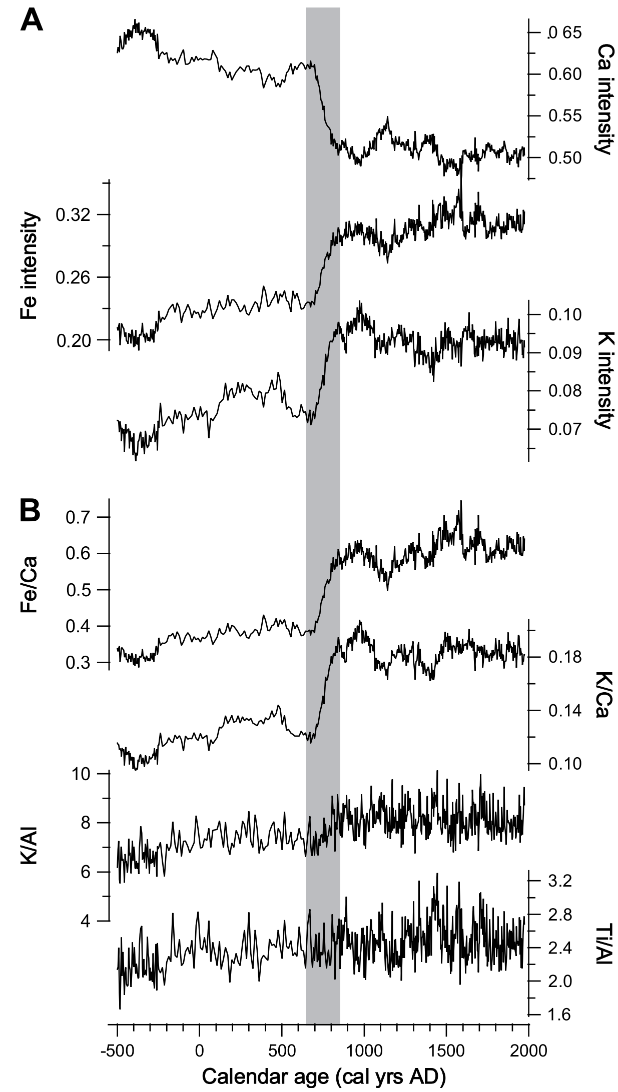

Fig. 2. Down-core XRF results for GeoB 6008-1 versus age. (A) Normalised element intensities for Ca, Fe, and K. (B) XRF Fe/Ca, K/Ca, K/Al, Ti/Al element ratios. Grey bar highlights the timing of the decrease in Ca and the increase in Fe and K between 650 and 850 AD. This shift is not seen in Al ratios suggesting the change in Fe/Ca and K/Ca is not related to increased chemical weathering or higher aeolian input.

The end-member algorithm (Weltje, 1997) was applied to particle size results from GeoB 6008-1 and GeoB 6008-2 to unmix the particle size distributions of the terrigenous sediment fraction into sub-populations, which are consequently interpreted in terms of transport mechanisms (see Section 3.3). Nine models were calculated with between 2 and 10 end-members per model and 59 size classes were considered (Fig. 3C). The simplest model, the two end-member model ($r^2_{mean} = 0.81$; Fig. 3D), shows very low r^2 of ~0.1 for the size range 10–12 μm, and a low r^2 for the <0.7 μm size classes (Fig. 3C). The three end-member model, the next simplest model, has a higher r^2_{mean} than the two end-member model ($r^2_{mean} = 0.91$; Fig. 3D), and shows high r^2 of >0.8 for most size classes, including for 10–12 μm (although r^2 is also low for the <0.7 μm size classes ($r^2 = 0.77$; Fig. 3C). The goodness-of-fit statistics suggest that the three-end-member model provides the best compromise between the number of end-members and r^2 per size class.

The particle size distributions of the three end-members are shown in Fig. 3E. The three end-members each have a clearly

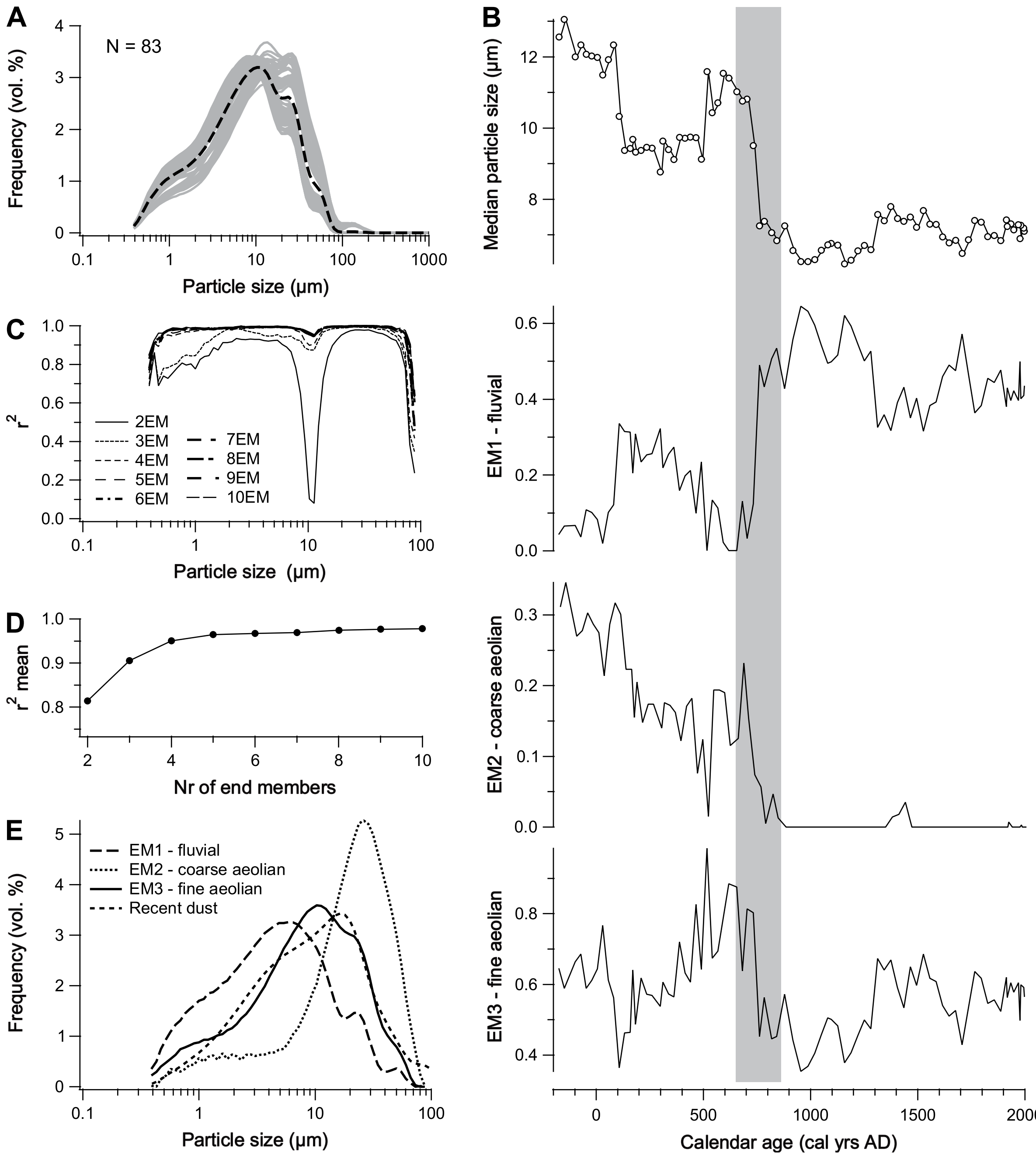

Fig. 3. Particle size and end-member modelling results for cores GeoB 6008-1 and GeoB 6008-2. (A) Particle size frequency distribution for each sample (grey lines), and average particle size frequency for the entire dataset ($n = 83$; dashed black line). (B) Median particle size changes through time, and the corresponding modelled end-member scores representing the proportions of fluvial (EM1), course aeolian (EM2), and fine aeolian (EM3) sediment components. (C) r^2 (goodness-of-fit) of models with 2–10 end-members for each particle size class. (D) Mean coefficient of determination (r^2_{mean}) of all size classes for each end-member model. (E) Comparison of particle size distributions for the end-members from the three end-member model with present-day dust collected nearby Site GeoB 6008 (Stuut et al., 2005).

defined, near-unimodal particle-size distribution. The first end-member (EM1) has a modal particle size of ~5 μm, the second end-member (EM2) of ~26 μm and the third end-member (EM3) has a modal particle size of ~10 μm. The end-members are interpreted as fluvial mud (EM1), 'coarse' aeolian dust (EM2), and 'fine' aeolian dust (EM3). Although there are no measurements of river suspended load for Morocco, the median grain size for sediment load from the Senegal River mouth is <10 μm (Gac and Kane, 1986), comparable to the median grain size of EM1 in the Site GeoB 6008 sediment cores, supporting the interpretation of EM1 as representing fluvial inputs. The fluvial inputs to Site GeoB 6008 are probably from ephemeral rivers draining the southern High Atlas Mountains and the catchment of the Tensift River (Fig. 1B). The particle size distributions of EM3 compares very well with data from present-day dust collected nearby our core location (Stuut et al., 2005) confirming the interpretation of EM3 as a fine wind-blown dust end-member (Fig. 3E). Sr–Nd isotopic studies of lithic particles in surface sediment cores from northwest Africa suggest aeolian input into our core location originates from the Middle and High Atlas region (Grousset et al., 1998). The interpretation that proximal aeolian dust (e.g. EM2) can be coarser grained than river-derived sediments is justified by the relatively short distance (few hundreds of kilometres) to the source of the wind-blown sediments.

The down-core proportions of the aeolian and fluvial populations are plotted against sediment age to reconstruct the regional sediment transport patterns in northwestern Africa during the past ~2000 years (Fig. 3B). The end-member ratios suggest that the shift in particle size between 650 and 850 AD is predominantly due to an increase in the fluvial component, EM1, and this suggests increased fluvial input (higher river sediment load) to the Site (Fig. 3B). The other two end-members (EM2 and EM3; coarse and fine aeolian dust, respectively) show a pronounced decrease at this time; the coarse aeolian end-member (EM2) shows a marked decrease between 650 and 850 AD to practically zero towards the present, and the fine aeolian end-member (EM3) is variable over the entire length of the core albeit with relatively low amplitude.

4.3. Total pollen and dinoflagellate cyst concentration and flux

Pollen and dinoflagellate cysts are particles of comparable chemical composition and size class, but have different origins. The concentration of pollen in the sediment mainly depends on the pollen production on land and on transport of the pollen, while cyst concentrations depend on their production in the overlying surface waters. Both are susceptible to oxygenic degradation but that should not be an issue here, due to the high sedimentation rates.

Total pollen concentration in GeoB 6008-1 ranges between 2.5×10^3 and 13.5×10^3 grains/ml, with maximum values found in sediments dated just before 600 AD, and from 700 to around 900 AD (Fig. 4A). Total pollen flux by contrast shows a marked increase from <300 to 1500 grains per centimetre squared per year (grains/cm^2/a) between 650 and 850 AD (Fig. 4B). The increased pollen flux is similar in timing to changes in the sedimentation rate (Fig. 4C). The higher pollen flux after 850 AD is sustained for the next 1000 years with only a slight decrease from 1700 AD to present. Over the length of the core the dinoflagellate cyst flux steadily increases from, on average, 600 cysts/cm^2/a to 9000 cysts/cm^2/a.

Between 650 and 850 AD the pollen flux increases in concert with the increase in sedimentation rate, while the pollen concentration remains steady. The steady pollen concentration suggests that pollen production on land has not changed (by contrast if pollen production had increased, assuming no other change, then the concentration (proportion) of pollen per millilitre of sediment would have increased). Instead, the increase in pollen flux suggests that more pollen is reaching Site GeoB 6008 because of the increase in terrestrial sediment (i.e. higher sedimentation rate), in which the pollen is entrained, delivered to Site GeoB 6008. This strongly suggests a land use driver for the 650–850 AD changes.

Changes in only the terrestrial system, from 650 to 850 AD, is further supported by the cyst concentration and flux results. The cyst concentration in the sediment falls between 600 and 1000 AD (Fig. 4A) proportionally with the rise in sedimentation rates (Fig. 4C) resulting in more or less stable cyst flux rates during this period (Fig. 4B), i.e. the production of cysts across the 650–850 AD transition is not related to the increase in sedimentation rate.

After 1000 AD the cyst concentration and flux both increase. This could be due to increased cyst productivity related to changes upwelling intensity observed at the core Site (McGregor et al., 2007), or could be related to increased fertilization from the higher amounts of terrestrial material reaching Site GeoB 6008.

4.4. Reproducibility

Results presented thus far from gravity core GeoB 6008-1 define abrupt changes occurring almost synchronously between approximately 650 and 850 AD. The abrupt shift is defined by a number of different parameters, including sediment composition (Ca, Fe, and K intensities and pollen flux; Fig. 2 and Fig. 4, respectively), sediment size (median particle size, fluvial and aeolian end-members; Fig. 3) and sedimentation rate (Fig. 4). This suggests that the change is a robust feature of the core, and that it represents a broader increase in the amount of terrestrial material supplied to Site GeoB 6008.

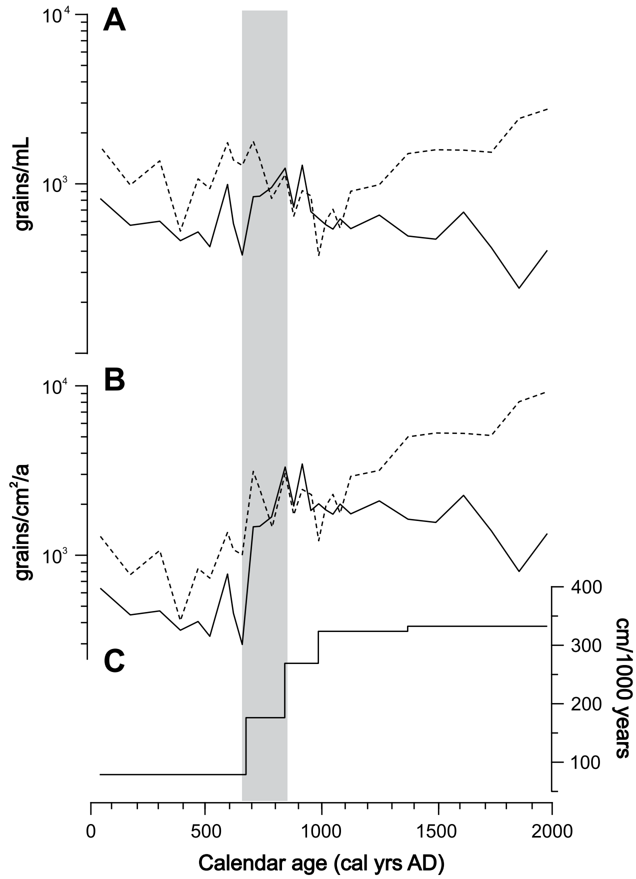

Fig. 4. Comparison of pollen and dinoflagellate cyst concentration and flux data with the sedimentation rate for core GeoB 6008-1. (A) Pollen (solid line) and dinoflagellate cyst (dashed line) concentrations on a logarithmic scale against age. (B) Pollen (solid line) and dinoflagellate cyst (dashed line) fluxes on a logarithmic scale. (C) Down-core sedimentation rate. The grey box highlights the period of changing sedimentation rate.

To test the regional extent and reproducibility of changes seen in GeoB 6008-1 from 650 to 850 AD we compared our results to the available data from the neighbouring gravity core GeoB 6007-2. GeoB 6007-2 is located offshore and in deeper water (30°51.0′ N, 10°16.1′ W, 900 m water depth; Neuer and cruise participants, 2000), from GeoB 6008-1 (Fig. 1B), and extends back to 14,000 years BP with an average sedimentation rate of about 120 cm/1000 years (Kuhlmann et al., 2004b). Despite these differences, GeoB 6007-2 also shows an abrupt shift, to increased Fe, occurring almost simultaneously with the increase in Fe in GeoB 6008-1 (Fig. 5A). Both sediment cores receive terrestrial material from the same source region and the Fe in both cores is assumed to come from the same source (Fig. 1B). Similarly, end-member modelling of GeoB 6007-2 also shows an increased fluvial component (Holz et al., 2007) as is seen in GeoB 6008-1 (Fig. 5B). This is a surprising result given that particle size for GeoB 6007-2 was determined using only the <63 μm size fraction (Holz et al., 2004) whereas the full range of particle size classes was measured for GeoB 6008-1. Together these results suggest that the 650–850 AD change is a characteristic event in this region and signifies a real change in the catchments and terrestrial environment of the southern High Atlas.

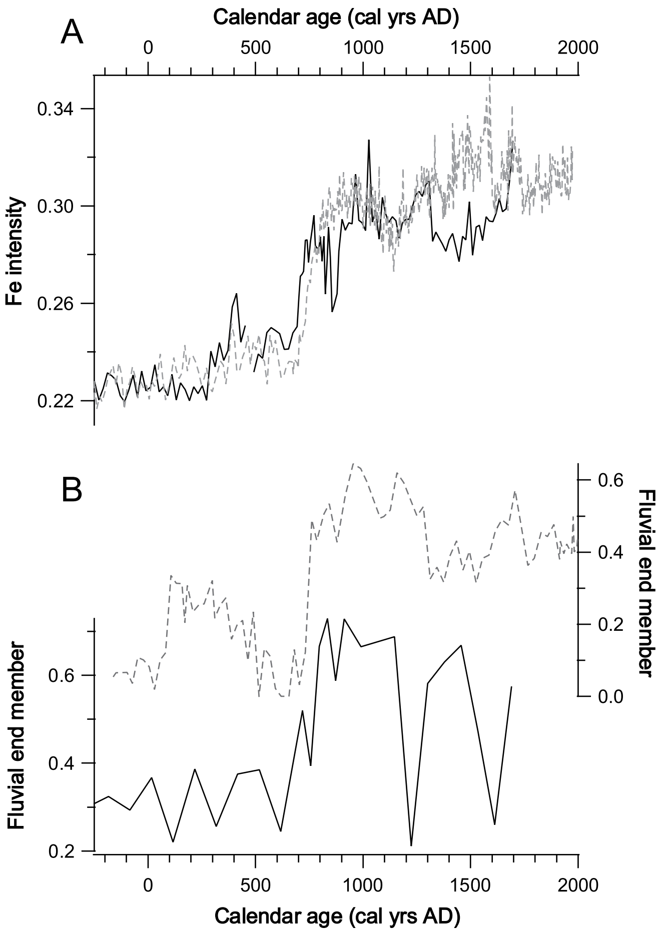

Fig 5. Comparison of Fe intensity and fluvial end-members between cores GeoB 6008-1 and GeoB 6007-2. (A) Fe intensity in sediment cores GeoB 6008-1 (dashed line) and GeoB 6007-2 (solid line) over the last 2000 years. Both cores show a rapid shift to increased Fe intensity at 650–850 AD (equivalent to 1300–1100 ca yr BP). (B) Fluvial end-members for cores GeoB 6008-1 (dashed line) and GeoB 6007-2 (solid line; data after Holz et al. (2007) and available at www.pangaea.de. doi:10.1594/PANGAEA.665698). Both cores show a shift in the proportion of the fluvial end-member beginning at around 650 AD.

4.5. Pollen taxa

Pollen data derived from marine sediments integrate palynological information of regional to continental areas in contrast to those data from most terrestrial deposits (e.g. lakes, bogs), which show local developments. Transport of pollen from their source areas to the marine sediments is also important. Aeolian transport of pollen predominates in deep-sea sediments located far from the coast and along arid areas with no or small river discharge, whereas fluvial transport is most important in humid low and mid latitudes, off river estuaries and in delta areas (Dupont, 1999). Thus, in interpreting the pollen results from Site GeoB 6008 a large geographical area was considered as the possible sources of the pollen grains found in the marine sediments. The area comprises the Mediterranean and Saharan vegetation zones as well as the transition zone in between, as shown in Table 1.

The total pollen percentages for a selection of pollen taxa are given in Fig. 6. In addition, the distribution of pollen taxa in ocean present-day (core-top) sediments off NW Africa were used to delineate possible pollen sources (Fig. 7). Four sections (pollen zones I–IV) were defined based on major changes in the pollen data (Fig. 6).

Pollen zone I includes eight samples dated from 50 to 650 AD. Cichorioideae pollen is the most abundant pollen type (10–18%) in pollen zone 1, and this zone has the highest percentages of pollen from *Pinus* (1–4%), *Q. robur/pubescens*-type (3–6%), *Juniperus/Tetraclinis* (0–3%), *Q. cerris/ilex*-type (0–4%), *Olea/Phillyrea* (1–4%), *Pistacia* (2–6%), and *Ephedra* (2–5%), compared to the rest of GeoB 6008-1.

Percentages of Cichorioideae pollen are remarkably high and are similar to levels found in peat and clay deposits from the western High Atlas Mountains (Reille, 1976). However, Cichorioideae pollen can be over-represented in some sediment deposits relative to their actual abundance because their thick exine (part of the pollen wall that fossilises) may enhance their preservation (Havinga, 1964). However, pollen of pine shows better preservation characteristics than Cichoroideae (Havinga, 1964). Thus, if Cichorioideae were represented in the core due to preferential preservation then *Pinus* pollen would also be expected to show similar trends to Cichorioideae. In core GeoB6008-1 Cichorioideae pollen are at high levels and increase toward the present, whereas *Pinus* pollen levels decline.

A large number of plant species contribute Cichorioideae pollen making it difficult to distinguish taxa to genus level. However, in modern marine sediments Cichorioideae pollen has the highest abundance at Site GeoB 6008 suggesting a local source for this pollen (Fig. 7). A likely local source is the argan scrub forest vegetation zone, onshore from Site 6008 (Fig. 1; Table 1), for which Cichorioideae pollen is associated, and a likely major producer of the Cichorioideae pollen is *Launaea arborescens*, a shrub species regularly found in degraded argan scrub forest sites of the western High Atlas (Culmsee, 2004).

The maximum *Pinus* value of 4% for pollen zone I is relatively low compared to other marine sediment cores from northwest Africa (although is the highest for *Pinus* in core GeoB6008-1). *Pinus* is generally a prolific pollen producer, so these low values likely indicate long distance pine pollen transport, possibly from as far as the Rif Mountains and the Middle Atlas, where pine trees are more abundant (Benabid, 1985; Hooghiemstra et al., 1992).

The percentage of *Quercus robur/pubescens*-type and *Q. cerris/ilex*-type, and *Ephedra* (combined *E. fragilis*-type and *E. distachya*-type) pollen in pollen zone I are the highest representations of these taxa in the core, and suggest both extensive oak forest and steppe vegetation. This is a paradox as it is unlikely these vegetation types are co-located and will be returned to in Section 5. The other pollen taxa indicate the presence of the Mediterranean bushland and thicket vegetation.

Pollen zone II includes seven samples dated between 650 and 950 AD. Relative pollen abundances of *Pinus* (0–3%) and *Quercus* (*Q. robur/pubescens*-type 1–3%, *Q. cerris/ilex*-type 2–4%) decline, those of *Juniperus/Tetraclinis* (0–3%) decline slightly. There is a gradual decline in *Ephedra* pollen from 4% to 1%. Values for *Olea/Phillyrea* (3–4%) and *Pistacia* (3–6%) remain at the same level. Pollen percentages increase for *Plantago* (0–1%) and *Artemisia* (1–3%). Cichorioideae shows a sharp rise of 10% to 20% beginning at 650 AD. The representation of *Argania spinosa* rises slightly from 2% to a maximum of 4% by the end of the 9th Century AD.

Pollen zone III includes 11 samples aged between 950 and 1800 AD. The most conspicuous feature of this part of the sequence is the continued high relative amounts of Cichorioideae pollen (average of 20%). Only the last sample (~ 1700 AD) is low in Cichorioideae. The trend to increased *Plantago* (0–2%) and *Artemisia* (2–4%) pollen is also continued. The representation of evergreen oaks (0–4%) remains steady. Other forest elements have generally low percentages. Pollen percentages of *Argania spinosa* from increase 3% to 8% beginning at around 950 AD and remain high throughout this period. The regular occurrence of pollen grains from Plumbaginaceae, *Calligonum*, and *Euphorbia* is noted.

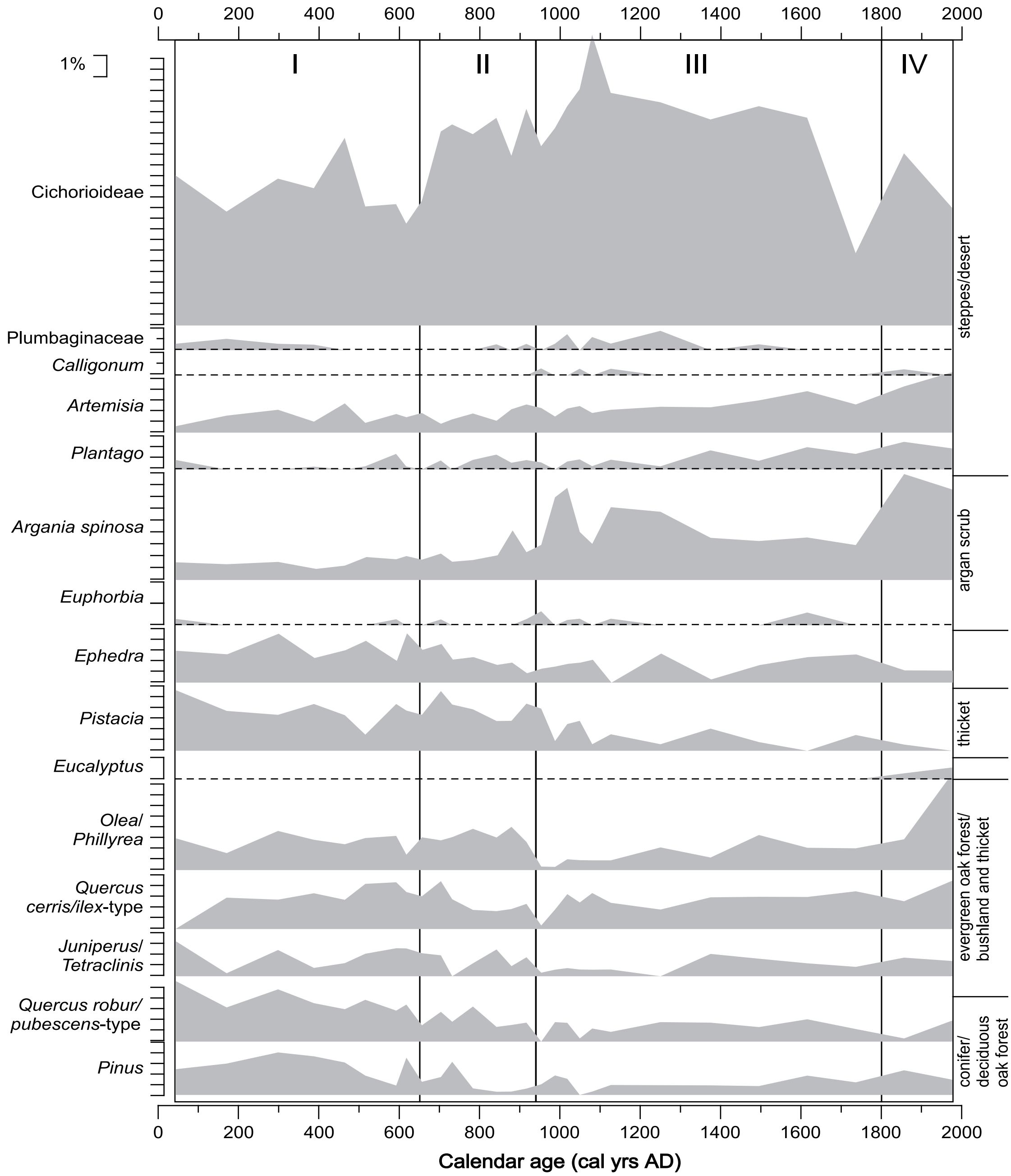

Fig. 6. Percentages of total pollen in core GeoB 6008-1 for selected taxa. Taxa have been grouped by their associated vegetation zones (right-hand side of figure) given in Table 1. The major tick interval is 1%. Numerals I–IV represent distinct pollen zones discussed in Section 4.5.

Pollen zone IV consists only of the upper two samples, dated after 1800 AD. This zone is characterised by maximum percentages for *Artemisia* (6%), *Plantago* (3%), *Argania spinosa* (9%), and *Olea/ Phillyrea* (9%). In addition, pollen grains of *Eucalyptus*, introduced from Australia, have been found. The *Eucalyptus* pollen thus reinforces our age model that this core extends into the most recent centuries. The upper part of the sequence most likely reflects the agricultural practice in the latter two centuries.

5. Discussion

5.1. Comparison of proxy data shifts from 650 AD

Several proxy records from core GeoB 6008 suggest a marked change beginning at around 650 AD. Levels of Cichorioideae, *Artemisia* and *Pantago* pollen increase and deciduous oak and *Ephedra* pollen decrease (Figs. 6 and 8). Sedimentation rate, Fe/Ca and pollen flux all increase, indicating increased terrestrial input to the Site (Fig. 8). The particle size end-member modelling suggests that the higher amount of terrestrial material is due to increased fluvial input (increased EM1, Fig. 8). The fluvial end-member is generally interpreted as an indicator of precipitation or moisture balance for a given region. However, the fluvial end-member actually reflects the sediment load of the rivers reaching the ocean. Increased sediment load is governed by erosion on land, which could be driven by climatic or land use change. A climate of higher precipitation and/or runoff could increase erosion, or a dryer climate could lead to an opening up of the vegetation making the land more susceptible to erosion. Land use change could directly increase erosion or could also lead to more

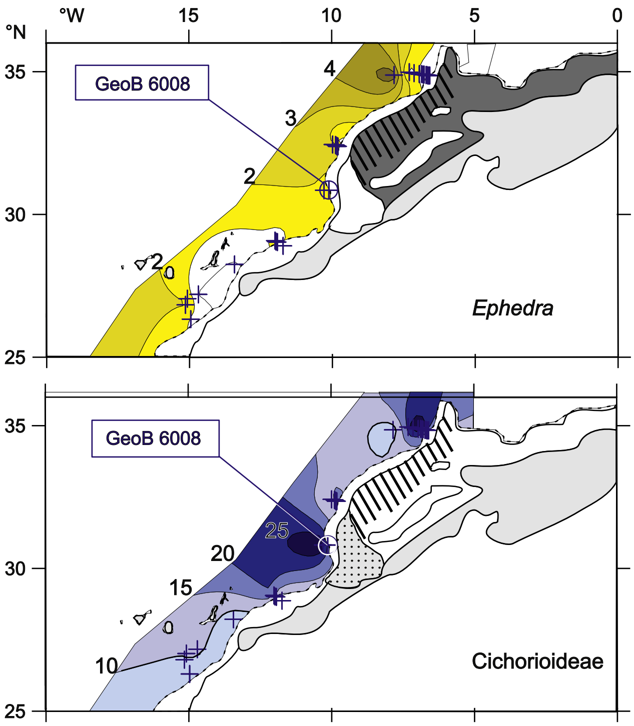

Fig. 7. Maps of the percentage distribution of *Ephedra* (*E. fragilis*-type and *E. distachya*-type) and Cichorioideae pollen in modern marine sediments, and the corresponding NW African pollen source area vegetation zones (shading as in Fig. 1C). Crosses represent the sediment core locations used to determine the modern marine pollen percentage distributions. Contouring is by Kriging interpolation (data after Hooghiemstra et al. (1986) and unpublished results available at www.pangaea.de). The NW African vegetation zones are as defined in Fig. 1C.

open vegetation structure and increase sediment availability. These two scenarios, (1) climate/precipitation change and (2) land use change, are discussed below with the data from Site GeoB 6008 used to test each scenario.

5.1.1. Scenario 1: climate/precipitation origin for the 650 AD shift

Under the climate/precipitation scenario the 650–850 AD shift suggests a rapid change from one climate mode to another. That is, before 650–850 AD aeolian deposition dominates and implies that more arid conditions prevail. After 650–850 AD fluvial deposition dominates and implies more or less consistently wetter conditions through to the present day. Since precipitation in Morocco is controlled by the large-scale North Atlantic Oscillation atmospheric circulation (Knippertz et al., 2003), the 650–850 AD 'mode shift' suggests a reorganisation of this large scale feature. A somewhat analogous scale shift could be the transition out of the "African Humid Period" at 6 ka BP (deMenocal et al., 2000).

Such a reorganisation in atmospheric circulation and increase in precipitation would likely be detected by other Moroccan paleoclimate records, particularly in records from the Atlantic side of the Atlas Mountains and the Atlantic coastal plains, since precipitation in these regions is dominated by NAO variability (Knippertz et al., 2003; Pauling et al., 2006). However, ostracod records of lake level changes for the Middle Atlas suggest no major change in precipitation over the last several thousand years (Barker et al., 1994; Lamb et al., 1995, 1999). Furthermore, pollen records, also from the Middle Atlas, show a steady decrease in precipitation over the past 2000 years, though the latter part of this reconstruction might be influenced by anthropogenic vegetation changes at the site (Cheddadi et al., 1998). Finally, for the past 1000 years the small changes that have occurred in the fluvial end-member do not

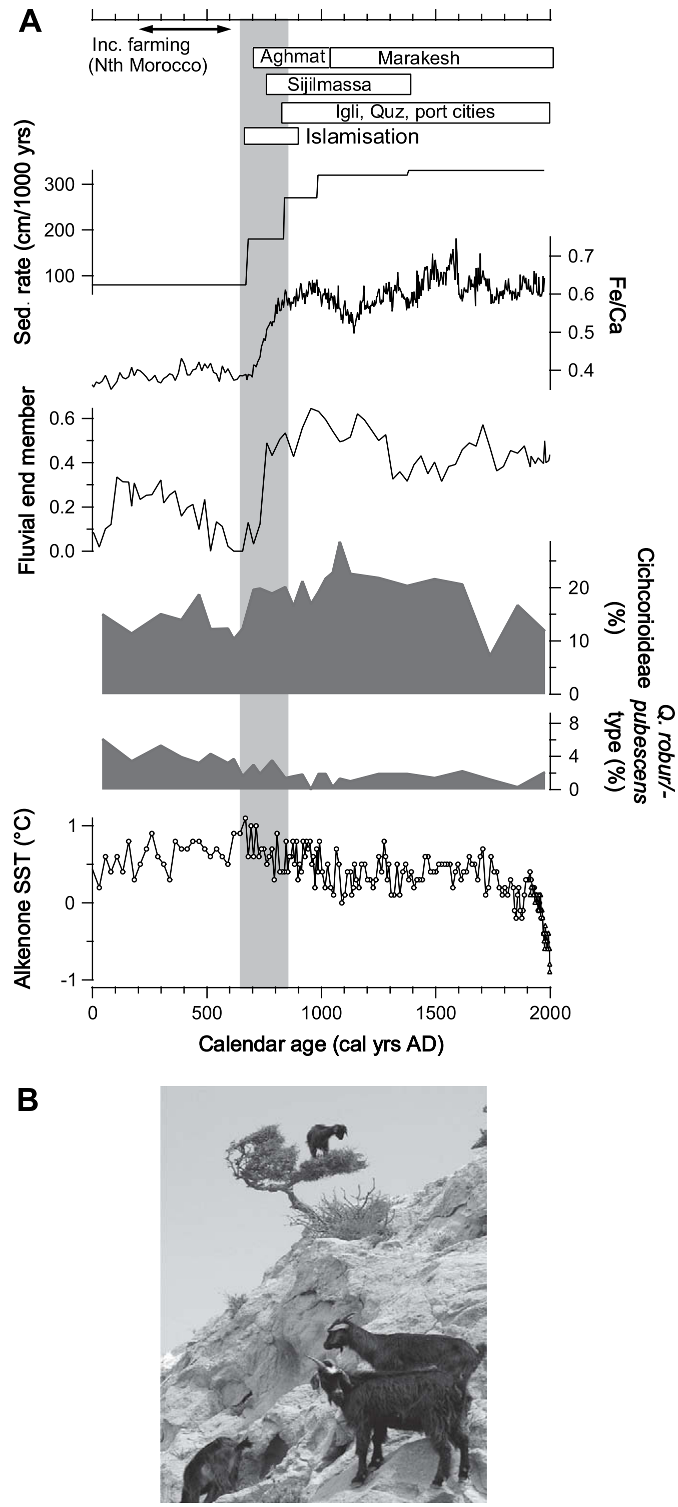

Fig. 8. (A) summary of sedimentation, XRF, particle size and pollen data for GeoB 6008-1, which define an abrupt change between 650 and 850 AD, and compared with alkenone SST anomalies (bottom) at Site 6008 (McGregor et al., 2007; data available at www.pangaea.de. doi:10.1594/PANGAEA.603183. doi:10.1594/PANGAEA.603185), and with selected Moroccan historical events (top) discussed in the text. (B) Goats as agents of change in southern Morocco. Image shows goats in an eroded landscape, and in the background a goat climbing an argan tree in search of fruit and fodder (photo courtesy of Robbie Morrison, Ottawa, Canada).

appear to relate to changes over the same period in Moroccan precipitation or Palmer Drought Severity Index, as reconstructed from northern Moroccan tree ring-widths (Till and Guiot, 1990; Esper et al., 2007). Thus there appears to be no clear link between precipitation and the increase in fluvial input into the southern Moroccan marine environment.

Although unlikely, precipitation in southern Morocco could be de-coupled from that in the rest of Morocco if local processes, such as upwelling-derived moisture, rather than large-scale processes dominated the signal. Upwelling is a major oceanic feature along the southern coast of Morocco and upwelling of cool waters, and the associated cooling of the atmosphere above, can be a major source of moisture to regions immediately onshore from the upwelling (Snyder et al., 2003). The alkenone sea surface temperature (SST) record from Site GeoB 6008 (Fig. 8) is a proxy for upwelling intensity (McGregor et al., 2007). This record, however, shows no major shift between 650 and 850 AD, with average values for this period similar to those for the proceeding $\sim$500 years. In addition, cyst flux (Fig. 4) show little change between 700 and 1000 AD, further suggesting limited changes in the local maritime climate. The alkenone SST and cyst records do not support the climate interpretation of the end-member results.

If precipitation had changed between 650 and 850 AD, then this would be expected to cause changes in the southern Morocco pollen record, since even small changes in water availability would have a large impact on the vegetation in this region. The decline of *Q. robur/pubescens*-type pollen percent (deciduous oak) and the relatively stable *Olea/Phillyrea* and *Pistacia* records suggest drier conditions. *Olea/Phillyrea* and *Pistacia* pollen, sourced from sclerophyllic trees, often reflect semi-arid conditions (Barbero et al., 1990; Hooghiemstra et al., 1992). The increase in *Artemisia* and *Plantago* pollen percentages also suggest drying as they represent drier steppe environments (Table 1).

The GeoB 6008-1 pollen record however, contains some paradoxes that are difficult to explain with a climate-only interpretation. For example, a drier climate should lead to a reduction in both deciduous oak and evergreen oak. While both appear to decline after 650 AD, the evergreen oak pollen percent rebound at $\sim$950 AD and remain stable or slightly increase up to present (Fig. 6). Deciduous oak percentages remain very low. Wetter conditions could explain the evergreen oak record however, this interpretation is not consistent with the pollen taxa changes described above.

In another contradiction, the GeoB 6008 pollen results show a highly unusual decline in the representation of both *Ephedra* and deciduous oaks. *Ephedra* and deciduous oaks are unlikely to occur together. *Ephedra* occurs in steppes and in the drier parts of the Mediterranean vegetation zone, so in a climate-only interpretation a decline in this pollen percent would suggest wetter conditions. Deciduous oaks occur in more humid forests of the Mediterranean vegetation zone, and a decline in deciduous oak pollen percentage would suggest drier conditions (as outlined above).

In summary, a climate-based interpretation does not adequately explain the 650–850 AD abrupt increase in fluvial input to Site GeoB 6008. There are no large-scale changes in precipitation that coincide with the shift and local changes in moisture balance cannot explain the results. In addition, the pollen record from Site GeoB 6008 does neither indicate an increase in taxa adapted to wetter conditions, nor does it suggest ubiquitously drier conditions from 650 AD onwards.

5.1.2. Scenario 2: land use origin for the 650 AD shift

Under scenario 2 the increase in fluvial input between 650 and 850 AD would be due to a change in land use and would lead to increased erodibility of the land or an increase in the area of erodible land. Soil erosion can increase by an order of magnitude or more due to increased cropping and livestock grazing and this translates to increased river sediment load and delivery to the ocean (Walling and Webb, 1996; Dearing and Jones, 2003). Sediment delivery shows a five- to tenfold increase as a result of human impacts and land use change (Dearing and Jones, 2003). The sedimentation rate for GeoB 6008-1 shows a threefold increase from 650 to 850 AD (Fig. 8) and is consistent with increased erosion on land, as is the increased Fe input (terrestrial material), and the increased pollen flux to Site GeoB 6008. If land use did change from 650 AD, the questions then become: are the changes in pollen taxa consistent with this interpretation, and what would drive the changes in land use?

The increased terrestrial/fluvial input in GeoB6008-1 for southern Morocco begins just prior to, but within error of, the Arab Islamic invasion of Morocco, a period associated with large-scale cultural, political and social upheaval (Brett, 1992; Brett and Fentress, 1996). The Arab invasion of north Africa began in the 660s AD and reached Tangier in northern Morocco in 711 AD. The invasion was initially confined to north of the former Roman frontier, the fortified *limes* that stretched right across north Africa at a longitude of about 34° N. Having reached Tangier, the Arabs quickly struck out for the desert fringe of southern Morocco and were the first invaders to reach the Souss River region (Fig. 1B) and the Tafilalt oasis, east of present-day Marrakech, over the High Atlas, and on their southern slopes (Abun-Nasr, 1971; Brett, 1992; Brett and Fentress, 1996). A key motivator for the Arab expansion into southern Morocco was probably the prospect of economic and commercial gain from the long-distance slave and gold trade with sub-Saharan Africa and the silver mining prospects in the Anti-Atlas Mountains (Brett, 1992). Despite the reluctance of the native Berber tribes of southern Morocco to accept Arab rule there is good evidence for significant development of southern Morocco around the time of, and just prior to, Islamisation (Abun-Nasr, 1971; Brett, 1992; Brett and Fentress, 1996). It appears that Aghmat, near to present-day Marrakech, was established by the 7th Century. Sijilmassa was founded in 757 AD in the oasis Tafilalt and became the centre of the flourishing trans-Saharan slave and gold trade during the Middle Ages. Texts of medieval Arabic geographers put emphasis on the richness of Sijilmassa (Brett, 1992; Lightfoot and Miller, 1996; Levtzion and Hopkins, 2000). The town of Igli on the Souss River was established sometime during the reign of Morocco's second king (Idris II) from 803 to 828/829 AD, and at the same time a chain of port cities were founded along the Atlantic coast from Massa, south of Agadir, to north of Rabat and included towns at Safi, Mogodor, and Qūz at the mouth of the Tensift River (Brett, 1992). Trade routes linked Aghmat to Sijilmasa and Igli, and to other towns in the region and beyond (Brett, 1969, 1992; Brett and Fentress, 1996). Estimates suggest that the Moroccan population doubled after the arrival of the Arabs (McEvedy and Jones, 1978), and migration and colonisation increased the population of southern Morocco, and expanded the pastoral and agricultural base (Brett, 1992).

An increase in pastoralism and deforestation could better explain the change in the pollen taxa from 650 AD than a climate-only interpretation. Clearing of land for pasture and firewood (Moroccans depend on firewood and charcoal for fuel (Mikesell, 1960)), would reduce tree species, and the introduction of domestic animals, particularly goats, to the southern Moroccan region would explain the decline in deciduous oak, and relatively unchanged evergreen oak pollen percentages recorded in GeoB 6008-1. Evergreen oaks, such as *Q. ilex*, are known to vigorously re-sprout after browsing and/or cutting (Lamb et al., 1991), much more so than deciduous oak (and pine), meaning that these trees are more likely to survive browsing pressure and explaining the more constant evergreen oak pollen levels.

Furthermore, the increases in argan tree (*Argania spinosa*) pollen could relate to an increase in goats in southern Morocco. *Argania spinosa* (argan tree) is native to southern Morocco (Charrouf and Guillaume, 1999). The argan tree produces highly prized oil, extracted by hand from the nuts (Charrouf and Guillaume, 1999). Occurrence and use of the argan tree was first described by Leo Africanus in 1550, who reported for the southern Moroccan region that "There are a great many prickly trees which produce a fruit as large as the olives we get from Spain. In the local language, this fruit is called: "argan". It is used to make an oil, which smells dreadfully, but which is used for cooking and for lighting." (Africanus, 1550; C. DeRouvray pers. commun.). Here we can confirm that the species has been growing in the southern Morocco region for at least the past 2000 years and increased by 1000 AD. Goats in southern Morocco have a unique relationship with the native argan tree; the goats are famous for climbing up the tree and browsing on the argan fruit (Fig. 8B). When the goats eat the fruit the fleshy part is digested and the nut remains. Traditionally, the nut is collected by the farmers to produce argan oil (Charrouf and Guillaume, 1999), and this provides an incentive for farmers to preserve the tree (Mikesell, 1960).

The high pollen values of Asteraceae (including *Artemisia*, Cichorioideae, Asteroideae), grasses, and *Plantago* after 650 AD could indicate degradation. Grasses and Asteraceae species often invade after the destruction of forest due to grazing and browsing pressure (Barbero et al., 1990) and several *Plantago* species are typical for pastures (Benabid, 2000). Cichorioideae, the most common pollen type in the core, shows a rapid increase from 650 AD and reflects changes landward of Site GeoB 6008 (Fig. 7). Cichorioideae pollen comes from a large number of plants species many of them weeds, though as described in Section 4.5, *Launaea arborescens* is a likely source of Cichorioideae pollen. This shrub species is common in degraded argan scrub forest sites of the western High Atlas (Culmsee, 2004). Thus, the increase in Cichorioideae pollen from 650 AD is probably associated with land use changes and land degradation beginning at this time. The increase in Asteraceae and decrease in deciduous oak represent a structural change to the vegetation and a reduction in vegetation cover, since many Asteraceae taxa only cover the soil during favourable seasons. This sporadic vegetation cover makes the soil very susceptible to erosion.

Although a land use change interpretation explains the changes in Cichorioideae, grass, deciduous oak and evergreen oak species it does not fully explain the decline in *Ephedra* pollen from 650 to 805 AD. Although two *Ephedra* pollen types have been identified, *E. distachya*-type pollen is however barely represented in the GeoB6008 sequence, reaching 1% in only four non-coherent samples (between 600 and 1300 AD). Percentages of *E. fragilis*-type, show a clear trend from 4% at 300AD to 1% at 900AD. *Ephedra fragilis*-type, comprises pollen from *E. fragilis*, *E. altissima*, and *E. alata*. *E. fragilis* occurs on the Canaries, the Iberian peninsula, in Algeria and Morocco, and as far south as the northern edge of the Sahara. *E. altissima* occurs in steppe and semi-desert communities, dunes of the coastal areas, and in the NW African and central Saharan mountains. *E. alata* occurs on dunes and isolated granite mountains in the northern and western Sahara (Knapp, 1973; Agwu and Beug, 1982).

A clue to interpreting the changes in *Ephedra* percentages may come from *Ephedra* pollen spatial distribution in modern marine sediments off northwest Africa, which can indicate the most likely source region for pollen from these species. Generally, *Ephedra* pollen percentages are highest offshore from northern Morocco (Hooghiemstra et al., 1986) and show a marked reduction south of 31° N. Thus, *Ephedra* pollen is most likely sourced mainly from northern Morocco or southern Spain and most likely transported by wind to Site 6008. The decrease in *Ephedra* pollen from 650 to 850 AD might represent either a (1) change occurring in the *Ephedra* source area (the more northern parts of Morocco), (2) a reduction in wind transport of *Ephedra* pollen to Site GeoB 6008, as suggested by the reduction in coarse aeolian input to the Site (Fig. 3), or (3) *Ephedra* pollen may be reduced due to a relative increase in the regional (southern Morocco) pollen flux, for example due to increased erosion. Importantly, the change in *Ephedra* pollen may at least partially be due to land use changes.

The changes in pollen abundance described above suggest that domestic animals, such as goats, may be a primary driver of the changes in vegetation, and goats could also contribute directly to the increased sedimentation rate recorded in core GeoB 6008-1.

Observational studies of goat impacts suggest they are responsible for alteration and destruction of native vegetation and increased erosion rates, both directly by physical dislodgement of soil, and indirectly by decreased or changed vegetation through browsing, trampling, and soil structure changes by hooves (Bayne et al., 2004). The impact of goats on soil erosion was recently quantified, and showed that areas with 20 goats/km^2 had five times higher erosion rates than areas with no or very few goats (Bayne et al., 2004).

Livestock erosion rates are also exacerbated by steep terrain (Mwendera et al., 1997), and in the mountainous regions of Morocco goats are known to accelerate deforestation. Goats have devastated the vegetation in some areas, not only due to their insatiable appetite, but by their constant consumption of new growth (Mikesell, 1960). Deforestation and vegetation removal by goats is further exacerbated by farming practices whereby animals are kept to areas that can be traversed in just a few hours (Mikesell, 1960), contributing further to over-grazing and soil erosion. Overall, the introduction of goats to southern Morocco as a result of Islamisation and population increase could account for the changes seen in both vegetation and erosion rates at 650–850 AD at Site GeoB 6008.

5.2. Changes from 850 AD to 1800 AD

From 850 AD to 1800 AD the changes in pollen taxa, fluvial input, sedimentation rate, Fe and pollen input seen previously are maintained and cemented. The changes between 850 and 1800 AD strongly suggest continued degradation of the vegetation and are consistent with land-use during the Middle Ages. By the 11th Century the population of Aghmat had grown considerably and the Almoravid dynasty founded Marrakesh in 1070 AD. Marrakesh became the capital of Morocco and remained so until the 17th Century (Abun-Nasr, 1971), attesting to the continued development and importance of the southern Moroccan region.

Continued land degradation is suggested by the high levels of Cichorioideae pollen, possibly *Launaea* (see previous section), and the increasing pollen percentages of *Artemisia* and *Plantago*. Pistache trees (*Pistacia* sp.) are known to be devastated by the browsing of goat herds (Mikesell, 1960) and the decline in *Pistacia* pollen percent after ~950 AD suggests that goats are continuing to have a large impact on the vegetation. The occurrence of *Calligonum* and Plumbaginaceae (probably *Limonium* or *Limoniastrum*) indicate either aridification or desertification. The *Euphorbia* pollen grains may originate from *Euphorbia beaumeriana* which nowadays grows in the coastal argan scrub forest (Culmsee, 2004). The representation of *Argania spinosa* increases and evergreen oaks are the only forest species that do not decline.

The increase in *Argania spinosa* pollen percentage began at ~950 AD and occurred in at most 60 years. The increase in the representation of argan trees from 950 AD could represent the beginning and development of cultivation and exploitation of this tree, and because of its economic value, the trees may have been protected from over-grazing/browsing by goats.

5.3. The record from 1800 AD

The vegetation changes in the upper part of core GeoB 6008-1 likely reflect intensified agricultural practices and continued land degradation. The fourfold increase in olive pollen is consistent with reports of olive cultivation in mountain valleys below 1200 m and the prominence of this tree in Moroccan commercial agriculture (Parish and Funnell, 1999). *Eucalyptus* pollen grains bespeak the plantings of exotic eucalypt trees thought to have begun in Morocco in the 1890s (Fraval and Haddan, 1989). The rise in *Argania spinosa* pollen most likely represents an increase in pre-steppe scrub forest rather than increased agricultural interest, as economic exploitation of this tree is reportedly in decline (Charrouf and Guillaume, 1999).

Artemisia is regarded as an indicator of advanced land degradation, and where excessive grazing, browsing, and harvesting occurs *Artemisia* 'steppic' shrubs increasingly dominate (Barbero et al., 1990; Puigdefábregas and Mendizabal, 1998). Thus the highest *Artemisia* pollen values during the post 1800 period most likely reflect high levels of land degradation. The steady increase in *Artemisia* pollen percent after 950 AD, the generally high levels of Cichorioideae pollen since 650 AD, and the other changes in pollen values, suggest that land degradation in southern Morocco may have began much earlier than the 1800s.

Studies of changes in 20th Century river sediment yield suggest that sediment yields generally increase with increased population (Walling and Webb, 1996). Population in Morocco trebled during the 20th Century (Department of Economic and Social Affairs of the United Nations Secretariat, 2006); however, sediment core GeoB 6008-1 shows no equivalent change in the sedimentation rate (Fig. 8). This puzzling result could be explained by the construction of numerous dams in Morocco for irrigation and socio-economic purposes (Minoia and Brusarosco, 2006; AQUASTAT Programme, 2007). Dams serve as major sediment traps (Walling and Webb, 1996; Syvitski et al., 2005) and in Morocco reservoir sedimentation is reducing dam capacity by 0.5% annually (Joundi and Gabriels, 2006). For instance, in the Rif region of northern Morocco siltation has caused the complete infiltration of a number of dams during the 1990s (Faleh et al., 2005). Lalla Takerkoust dam on the N'tis river near Marrakesh has 28% less capacity than when it was commissioned in 1935 due to sedimentation (AQUASTAT Programme, 2007). It is possible that any increased 20th Century sedimentation is balanced by sediment accumulation behind dams along the Tensif and Ouem er Rbia Rivers (Minoia and Brusarosco, 2006), thus preventing additional sediment from reaching the ocean and Site GeoB 6008.

5.4. Implications for human–climate–environment interactions

The Kingdom of Morocco is highly vulnerable to the impacts of climate change (Kingdom of Morocco, 2001; Agoumi, 2003; Giorgi, 2006; Christensen et al., 2007). The region is expected to experience a large decrease in average rainfall, an increase in rainfall variability, and more frequent drought episodes in the future (Giorgi, 2006; Christensen et al., 2007). Large socio-economic consequences of rainfall changes are predicted, since approximately 40% of Morocco's population is dependent on the rain-dominated agricultural sector (US State Department, 2007). In addition, Morocco's rapidly increasing population, up 2.2% per year since 1950 (Department of Economic and Social Affairs of the United Nations Secretariat, 2006), has led to pressure on eco- and terrestrial systems, with the Moroccan landscape subject to land degradation and desertification (Messerli and Winiger, 1992; Puigdefábregas and Mendizabal, 1998; Parish and Funnell, 1999; Sobrino and Raissouni, 2000), deforestation (Mikesell, 1960), and ecosystem degradation (Barbero et al., 1990; Culmsee, 2004).

Desertification, the degradation of the land in arid and semi-arid regions, results from a combination of an arid climate, irregular seasons, poor soils and degradation of soils, deforestation by clearing, reduction of vegetation by foraging animals, high erosion rates, and population pressure. In Morocco, population has increased threefold since 1950, and agriculture is encroaching on rangeland at a rate of 1% per year (Puigdefábregas and Mendizabal, 1998). In addition, vegetation is becoming more steppic (indicating degradation), and is associated with an increase in erosion (Barbero et al., 1990). Future pressure on the landscape and ecosystem will come from complex socio-economic and climatic factors (Puigdefábregas and Mendizabal, 1998; Parish and Funnell, 1999). For example, increased temperatures as the result of global warming are expected to increase the upper cultivation boundaries in the mountain valley regions of the High Atlas landward of Site GeoB 6008-1 (Parish and Funnell, 1999). However, as these boundaries move up-valley, the available land reduces due to the steep terrain, requiring the costly construction of terraces and the extension of irrigation channels (Parish and Funnell, 1999). This expansion is labour intensive and strong incentives would be necessary to attract the required workforce. Increased demand for the agricultural produce would be strong enough to drive these changes, despite the high costs (Parish and Funnell, 1999). An increase in up-valley agriculture, however, if not managed properly, would result not only in reduced biodiversity but also in land degradation due to soil loss and erosion—also accelerated by more intense rainfall events (Giorgi, 2006).

Results from sediment core GeoB 6008-1 suggest that land degradation and erosion in southern Morocco may have a much longer history than the past 50 years, and that degradation and erosion processes may have begun as early as the 8th Century AD. Furthermore, the results show that there was no respite once the changes had begun, possibly indicating that an ecosystem/landscape threshold had been crossed. Based on evidence presented in this study, it should be possible to classify southwest Morocco in terms of its past vulnerability, then assess sensitivity/resilience to future impacts (Dearing, 2006). Knowing that southwest Morocco is already degraded and susceptible to very high erosion rates, and as pressure increases to push agriculture and pastoralism to new regions, soil stabilisation strategies, such as tree planting, restricting livestock (goat) browsing and foraging, especially on steep slopes, should be employed to prevent further land degradation.

Results from southern Morocco suggest that semi-arid regions (e.g. desert-loess margins in China, the Sahel, semi-arid Australia) in general may be highly vulnerable to human impact. The vegetation and land in semi-arid regions may therefore have reduced buffering capacity against future socio-economic and climate pressures, making it more sensitive to change and less resilient to increased soil erosion (Messerli and Winiger, 1992). Management and mitigation of land degradation and ecosystems in these regions must take into account the long history of vegetation change to properly establish ecosystem baselines, steady states, thresholds and resilience (Dearing, 2008; Froyd and Willis, 2008).

Finally, The results from GeoB 6008-1 also provide a cautionary note for the interpretation of marine sediment core palaeo-records from northwest Africa. Terrestrial proxies such as element intensities, particle size and pollen composition are often reconstructed over Quaternary time scales and compared with the uppermost samples representing the late Holocene. Our results suggest that the late Holocene period may have a strong anthropogenic overprint and terrestrial proxies from this period do not necessarily reflect climate alone. This point should be taken into account when interpreting longer-term records of Quaternary climate change from marine sediment cores for northwest Africa and elsewhere.

6. Summary and conclusions

Analysis of sediment core GeoB 6008-1 located off the coast of southern Morocco shows an abrupt increase in sedimentation rate, Fe intensity, and pollen flux between 650 and 850 AD, indicating increased deposition of terrestrial material at the Site. Particle size analyses and end-member modelling of the particle size distributions suggest that the terrestrial material increased due to increased fluvial input. The high levels of fluvial input are maintained from 850 AD up to the present day.

The abrupt rise in fluvial input to Site GeoB 6008 cannot be explained by climatic factors such as increased precipitation and/or runoff. The amount of rainfall needed for the shift would have changed the vegetation of the western High Atlas considerably; the pollen record from GeoB 6008-1 does not suggest wetter conditions. Instead, we interpret the fluvial input as an increase in terrestrial erosion.

The increase in terrestrial erosion is in turn attributed to increased habitation and herding of goats in southern Morocco. This would change the vegetation and increase erosion, leading to more fluvial input of fine grained material and increased pollen flux of scrub and steppic elements as is seen in the GeoB 6008 record. The environmental changes suggested here can be connected to the strong politic and economic development of southern Morocco that took place around 700 AD, the time of Islamisation of the indigenous people.

Results from this study suggest that the ecosystem and terrestrial environment in southern Morocco have been in a modified state, due to human-induced land use changes, for much of the last 1300 years. Prediction of the impact of future climate change, the management of catchments and pastoral-agricultural systems must take into account the long history of degraded vegetation for this region.

Acknowledgements

The authors would like to thank A. Kappel, C. Gonzalez and O. Lackmann for preparation of pollen samples, and J. Marthik for preparation of the location map. We thank G. Weltje for making available the end-member modelling algorithm. Thoughtful discussions with S. Mulitza, J. Kemp, M. Brett, I. Bouimetarhan, and A. Simms are gratefully acknowledged. J. Dodson, C. Murray-Wallace, and T. Schambron are thanked for constructive comments on early versions of the manuscript. This work was supported by funds from the EU PACLIVA Project, and through the DFG-Research Center/Excellence Cluster "The Ocean in the Earth System". Data from this study will be archived in the Pangaea World Data Center, www.pangaea.de.

References

Abun-Nasr, J.M., 1971. A History of the Maghrib. Cambridge University Press, Cambridge.

Africanus, L., 1550. Cosmographia Del Africa. Translation by Epaulard, A., 1956. Description de l'Afrique. Maisonneuve, Paris.

Agoumi, A., 2003. Vulnerability of north African countries to climatic changes: adaptation and implementation strategies for climatic change. Technical report, International Institute for Sustainable Development/Climate Change Knowledge Network, Winnipeg. http://www.cckn.net//pdf/north_africa.pdf.

Agwu, C.O.C., Beug, H.-J., 1982. Palynological studies of marine sediments off the West African coast. "Meteor" Forschungs-Ergebnisse C 36, 1–30.

Aquastat Programme, 2007. Dams and agriculture in Africa. Technical report, Water Development and Management Unit, Land and Water Division, Food and Agriculture Organization of the United Nations, Report No. FAO Aquastat Dams Africa—070524. http://www.fao.org/nr/water/aquastat/damsafrica/index.stm.

Arz, H.W., Lamy, F., Pätzold, J., Müller, P.J., Prins, M., 2003. Mediterranean moisture source for an Early-Holocene humid period in the northern Red Sea. Science 300, 118–121.

Barbero, M., Bonin, G., Loisel, R., Quézel, P., 1990. Changes and disturbances of forest ecosystems caused by human activities in the western part of the mediterranean basin. Vegetatio 87, 151–173.

Barker, P.A., Roberts, N., Lamb, H.F., van der Kaars, S., Benkaddour, A., 1994. Interpretation of Holocene lake-level change from diatom assemblages in Lake Sidi Ali, Middle Atlas, Morocco. Journal of Paleolimnology 12, 223–234.

Bayne, P., Harden, R., Davies, I., 2004. Feral goats (*Capra hircus* L.) in the Macleay River gorge system, north-eastern New South Wales, Australia. I. Impacts on soil erosion. Wildlife Research 31, 519–525.

Benabid, A., 1985. Les écosystemes forestiers, préforestiers et présteppiques du Maroc. Forêt méditerranéenne 7, 53–64.

Benabid, A., 2000. Flore et écosytèmes du Maroc: Evaluation et préservation de la biodiversité. Ibis Press, Paris.

Beug, H.-J., 2004. Leitfaden der pollenbestimmung. Pfeil-Verlag, Munich.

Brett, M., 1969. Ifriqiya as a market for Saharan trade from the tenth to the twelfth century A.D. Journal of African History 10, 347–364.

Brett, M., 1992. The Islamisation of Morocco from the Arabs to the Almoravids. Morocco 2, 57-71, Republished in Brett, M., 1999. Ibn Khaldun and the Medieval Maghrib. Variorum Collected Studies Series: CS627. Ashgate Publishing Ltd., Aldershot.

Brett, M., Fentress, E., 1996. The Berbers. Blackwell Publishing, Oxford.

Charrouf, Z., Guillaume, D., 1999. Ethnoeconomical, ethnomedical, and phytochemical study of *Argania spinosa* (L.) skeels: a review. Journal of Ethnopharmacology 67, 7–14.

Cheddadi, R., Lamb, H.F., Guiot, J., van der Kaars, S., 1998. Holocene climatic change in Morocco: a quantitative reconstruction from pollen data. Climate Dynamics 14, 883–890.

Christensen, J.H., Hewitson, B., Busuioc, A., Chen, A., Gao, X., Held, I., Jones, R., Kolli, R.K., Kwon, W.-T., Laprise, R., Magaña Rueda, V., Mearns, L., Menéndez, C.G., Räisänen, J., Rinke, A., Sarr, A., Whetton, P., 2007. Regional climate projections. In: Solomon, S., Qin, D., Manning, M., Chen, Z., Marquis, M., Averyt, K.B., Tignor, M., Miller, H.L. (Eds.), Climate Change 2007: The Physical Science Basis. Contribution of Working Group I to the Fourth Assessment Report of the Intergovernmental Panel on Climate Change. Cambridge University Press, Cambridge, UK and New York, USA.

Culmsee, H., 2004. Vegetation und Weidenutzung im Westlichen Hohen Atlas (Marokko). MSc Thesis, Cramer-Borntraeger, Stuttgart.

Dearing, J.A., Jones, R.T., 2003. Coupling temporal and spatial dimensions of global sediment flux through lake and marine sediment records. Global and Planetary Change 39, 147–168.

Dearing, J.A., 2006. Climate-human–environment interactions: resolving our past. Climate of the Past 2, 187–203.

Dearing, J.A., Battarbee, R.W., Dikau, R., Larocque, I., Oldfield, F., 2006. Human–environment interactions: learning from the past. Regional Environmental Change 6, 1–16.

Dearing, J.A., 2008. Landscape change and resilience theory: a palaeoenvironmental assessment from Yunnan, SW China. The Holocene 18, 117–127, doi:10.1177/0959683607085601.

deMenocal, P., Ortiz, J., Guilderson, T., Adkins, J., Sarnthein, M., Baker, L., Yarusinsky, M., 2000. Abrupt onset and termination of the African Humid Period: rapid climate response to gradual insolation forcing. Quaternary Science Reviews 19, 347–361.

Department of Economic and Social Affairs of the United Nations Secretariat, 2006. World Population Prospects: The 2006 Revision and World Urbanization Prospects: The 2005 Revision, Sept 2007 update.

Dupont, L.M., 1999. Pollen and spores in marine sediments from the east Atlantic–a view from the ocean into the African continent. In: Fischer, G., Wefer, G. (Eds.), Use of Proxies in Paleoceanography: examples from the South Atlantic. Springer, Berlin, pp. 523–546.

Esper, J., Frank, D., Büntgen, U., Verstege, A., Luterbacher, J., Xoplaki, E., 2007. Long-term drought severity variations in Morocco. Geophysical Research Letters 34, L17702, doi:10.1029/2007GL030844.

Faedri, K., Iversen, J. (Eds.), 1989. Textbook of Pollen Analysis, fourth ed. Wiley and Sons, Chichester.

Faleh, A., Navas, A., Sadiki, A., 2005. Erosion and dam siltation in a Rif catchment (Morocco). Sediment Budgets 2. IAHS Publications 292, 58–64.

Fraval, A., Haddan, M., 1989. Phoracantha. Actes Éditons, Rabat.

Frenz, M., Höppner, R., Stuut, J.-B., Wagner, T., Henrich, R., 2003. Surface sediment bulk geochemistry and grain-size composition related to the oceanic circulation along the south American continental margin in the southwest Atlantic. In: Wefer, G., Mulitza, S., Ratmeyer, V. (Eds.), The South Atlantic in the Late Quaternary: Reconstruction of Material Budgets and Current Systems. Springer, Berlin, pp. 347–373.

Froyd, C.A., Willis, K.J., 2008. Emerging issues in biodiversity & conservation management: the need for a palaeoecological perspective. Quaternary Science Reviews 27, 1723–1732.

Gac, J.Y., Kane, A., 1986. Le Fleuve Sénégal: I. Bilan hydrologique et flux continentaux de matières particulaires a l'embouchure. Sciences Géologiques Bulletin 39, 99–130.
Giorgi, F., 2006. Climate change hot-spots. Geophysical Research Letters 33, L08707, doi:10.1029/2006GL025734.
Grousset, F.E., Parra, M., Bory, A., Martinez, P., Bertrand, P., Shimmield, G., Ellam, R.M., 1998. Saharan wind regimes traced by the Sr–Nd isotopic composition of subtropical Atlantic sediments: Last Glacial Maximum vs today. Quaternary Science Reviews 17, 395–409.
Havinga, A., 1964. Palynology and pollen preservation. Review of Palaeobotany and Palynology 2, 81–98.
Holz, C., Stuut, J.-B.W., Henrich, R., 2004. Terrigenous sedimentation processes along the continental margin off NW Africa: implications from grain-size analysis of seabed sediments. Sedimentology 51, 1145–1154.
Holz, C., Stuut, J.-B.W., Henrich, R., Meggers, H., 2007. Variability in terrigenous sedimentation processes off northwest Africa and its relation to climate changes: inferences from grain-size distributions of a Holocene marine sediment record. Sedimentary Geology 202, 499–508, doi:10.1016/j.sedgeo.2007.03.015.
Hooghiemstra, H., Agwu, C.O.C., Beug, H.-J., 1986. Pollen and spore distribution in recent marine sediments: a record of NW-African seasonal wind patterns and vegetation belts. "Meteor" Forschungs-Ergebnisse C 40, 87–135.
Hooghiemstra, H., Stalling, H., Agwu, C.O.C., Dupont, L.M., 1992. Vegetational and climatic changes at the northern fringe of the Sahara 250,000–5000 years BP: evidence from 4 marine pollen records located between Portugal and the Canary Islands. Review of Palaeobotany and Palynology 74, 1–53.
Joundi, S., Gabriels, D., 2006. Empirical models for the assessment of specific sediment yields in reservoirs and large dams of Morocco. International Symposium on Drylands Ecology and Human Security. United Arab Emirates, Dubai. Abstract 2006/056.
Kingdom of Morocco, 2001. Initial national communication on the United Nations Framework Convention on Climate Change. Ministère de l'Aménagement du Territoire, de l'Urbanisme, de l'Habitat et de l'Environnement, p. 25.
Knapp, R., 1973. Die Vegetation von Afrika. Fischer, Stuttgart.
Knippertz, P., Christoph, M., Speth, P., 2003. Long-term precipitation variability in Morocco and the link to the large-scale circulation in recent and future climates. Meteorology and Atmospheric Physics 83, 67–88, doi:10.1007/s00703-002-0561-y.
Kuhlmann, H., Freudenthal, T., Helmke, P., Meggers, H., 2004a. Reconstruction of paleoceanography off NW Africa during the last 40,000 years: influence of local and regional factors on sediment accumulation. Marine Geology 207, 209–224.
Kuhlmann, H., Meggers, H., Freudenthal, T., Wefer, G., 2004b. The transition of the monsoonal and the N Atlantic climate system off NW Africa during the Holocene. Geophysical Research Letters 31, L22204.
Lamb, H., Roberts, N., Leng, M., Barker, P., Benkaddour, A., van der Kaars, S., 1999. Lake evolution in a semi-arid montane environment: responses to catchment change and hydroclimatic variation. Journal of Paleolimnology 21, 325–343.
Lamb, H.F., Damblon, F., Maxted, R.W., 1991. Human impact on the vegetation of the Middle Atlas, Morocco, during the last 5000 years. Journal of Biogeography 18, 519–532.
Lamb, H.F., Gasse, F., Benkaddour, A., El Hamouti, N., van der Kaars, S., Perkins, W.T., Pearce, N.J., Roberts, C.N., 1995. Relation between century-scale Holocene arid intervals in tropical and temperate zones. Nature 373, 134–137.
Levtzion, N., Hopkins, J.F.P., 2000. Corpus of Early Arabic Sources for West African History. First Markus Wiener Publishers, Princeton.
Lightfoot, D.R., Miller, J.A., 1996. Sijilmassa: The rise and fall of a walled oasis in Medieval Morocco. Annals of the Association of American Geographers 86, 78–101.
Martinez, P., Bertrand, P., Shimmield, G.B., Cochrane, K., Jorissen, F.J., Foster, J., Dignan, M., 1999. Upwelling intensity and ocean productivity changes off Cape Blanc (northwest Africa) during the last 70,000 years: geochemical and micropalaeontological evidence. Marine Geology 158, 57–74.
McEvedy, C., Jones, R., 1978. Atlas of World Population History. Penguin Books Ltd., London.
McGregor, H.V., Dima, M., Fischer, H.W., Mulitza, S., 2007. Rapid 20th-Century increase in coastal upwelling off northwest Africa. Science 315, 637–639, doi:10.1126/science.1134839.
Messerli, B., Winiger, M., 1992. Climate, environmental change, and resources of the African mountains from the Mediterranean to the equator. Mountain Research and Development 12, 315–336.
Mikesell, M.W., 1960. Deforestation in northern Morocco. Science 132, 441–448.
Minoia, P., Brusarosco, A., 2006. Water infrastructures facing sustainable development challenges: integrated evaluation of impacts of dams on regional development in Morocco. Technical report, NRM Natural Resources Management Working Papers, Fondazione Eni Enrico Mattei, Report No. (Nota di Lavoro) 105.06. http://ideas.repec.org/p/fem/femwpa/2006.105.html.
Moore, P.D., Webb, J.A., Collinson, M.E., 1991. Pollen Analysis, second ed. Blackwell Scientific Publications, London.
Mwendera, E.J., Mohamed Saleem, M.A., Dibabe, A., 1997. The effect of livestock grazing on surface runoff and soil erosion from sloping pasture lands in the Ethiopian highlands. Australian Journal of Experimental Agriculture 37, 421–430.
Neuer, S. and cruise participants, 2000. Report and preliminary results of Meteor Cruise M 45/5, Bremen-Las Palmas, October 1–November 3, 1999. Technical report, Berichte, Fachbereich Geowissenschaften, No. 163, Universität Bremen, Bremen.
Parish, R., Funnell, D.C., 1999. Climate change in mountain regions: some possible consequences in the Moroccan High Atlas. Global Environmental Change 9, 45–58.
Pauling, A., Luterbacher, J., Casty, C., Wanner, H., 2006. Five hundred years of gridded high-resolution precipitation reconstructions over Europe and the connection to large-scale circulation. Climate Dynamics 26, 387–405, doi:10.1007/s00382-005-0090-8.
Prins, M.A., Weltje, G.J., 1999. End-member modeling of siliciclastic grain-size distributions: the Late Quaternary record of eolian and fluvial sediment supply to the Arabian Sea and its paleoclimatic significance. In: Harbaugh, J., Watney, L., Rankey, G., Slingerland, R., Goldstein, R., Franseen, E. (Eds.), Numerical Experiments in Stratigraphy: Recent Advances in Stratigraphic and Sedimentologic Computer Simulations. Society for Sedimentary Geology, pp. 91–111.
Puigdefábregas, J., Mendizabal, T., 1998. Perspectives on desertification: western Mediterranean. Journal of Arid Environments 39, 209–224.
Quézel, P., 1978. Analysis of the Flora of Mediterranean and Saharan Africa. Annals of the Missouri Botanical Garden 65, 479–534.
Reille, M., 1976. Analyse pollinique de sédiments postglaciaires dans le Moyen Atlas et le Haut Atlas marocains: premiers résultats. Ecologia Mediterranea 2, 153–170.
Snyder, M.A., Sloan, L.C., Diffenbaugh, N.S., Bell, J.L., 2003. Future climate change and upwelling in the California Current. Geophysical Research Letters 30, 1823, doi:10.1029/2003GL017647.
Sobrino, J.A., Raissouni, N., 2000. Toward remote sensing methods for land cover dynamic monitoring: application to Morocco. International Journal of Remote Sensing 21, 353–366, doi:10.1080/014311600210876.
Stuut, J.-B.W., Prins, M.A., Schneider, R.R., Weltje, G.J., Jansen, J.H.F., Postma, G., 2002. A 300-kyr record of aridity and wind strength in southwestern Africa: inferences from grain-size distributions of sediments on Walvis Ridge, SE Atlantic. Marine Geology 180, 221–233.
Stuut, J.-B.W., Zabel, M., Ratmeyer, V., Helmke, P., Schefuß, E., Lavik, G., Schneider, R., 2005. Provenance of present-day eolian dust collected off NW Africa. Journal of Geophysical Research 110, D04202.
Syvitski, J.P.M., Vörösmarty, C.J., Kettner, A.J., Green, P., 2005. Impact of humans on the flux of terrestrial sediment to the global coastal ocean. Science 308, 376–380, doi:10.1126/science.1109454.
The Plant Press, 1997–2006. Dictionary of Common Names. The Plant Press Ltd. http://www.plantpress.com/dictionary.html.
Till, C., Guiot, J., 1990. Reconstruction of precipitation in Morocco since 1100 A.D. based on *Cedrus atlantica* tree-ring widths. Quaternary Research 33, 337–351.
US State Department, 2007. Background Note: Morocco. Bureau of Near Eastern Affairs, October 2007 update. http://www.state.gov/r/pa/ei/bgn/5431.htm#.
Walling, D.E., Webb, B.W., 1996. Erosion and sediment yield: a global overview. In: Walling, D.E., Webb, B.W. (Eds.), Erosion and Sediment Yield: Global and Regional Perspectives. IAHS Press, Wallingford, UK, pp. 3–19.
Weisrock, A., Wahl, L., Ouammou, A., Chakir, L., 2006. Systèmes fluviaux du Sud-Ouest marocain et leur évolution depuis le Pléistocène supérieur (Fluvial systems of southwestern Morocco and their evolution since the Late Pleistocene). Géomorphologie: Relief, Processus, Environnement 4, 229–248.
Weltje, G., 1997. End-member modelling of compositional data: Numerical-statistical algorithms for solving the explicit mixing problem. Journal of Mathematical Geology 29, 503–549.
Weltje, G.J., Prins, M.A., 2003. Muddled or mixed? Inferring palaeoclimate from size distributions of deep-sea clastics. Sedimentary Geology 162, 39–62.
White, F., 1983. The Vegetation of Africa: A Descriptive Memoir to Accompany the UNESCO/AETFAT/UNSO Vegetation Map of Africa. UNESCO, Paris.
Yarincik, K.M., Murray, R.W., Peterson, L.C., 2000. Climatically sensitive eolian and hemipelagic deposition in the Cariaco Basin, Venezuela, over the past 578,000 years: results from Al/Ti and K/Al. Paleoceanography 15, 210–228.
Zabel, M., Schneider, R.R., Wagner, T., Adegbie, A.T., de Vries, U., Kolonic, S., 2001. Late Quaternary climate changes in central Africa as inferred from terrigenous input to the Niger Fan. Quaternary Research 56, 207–217.